The Universe in X-rays: telescopes, observations and theory

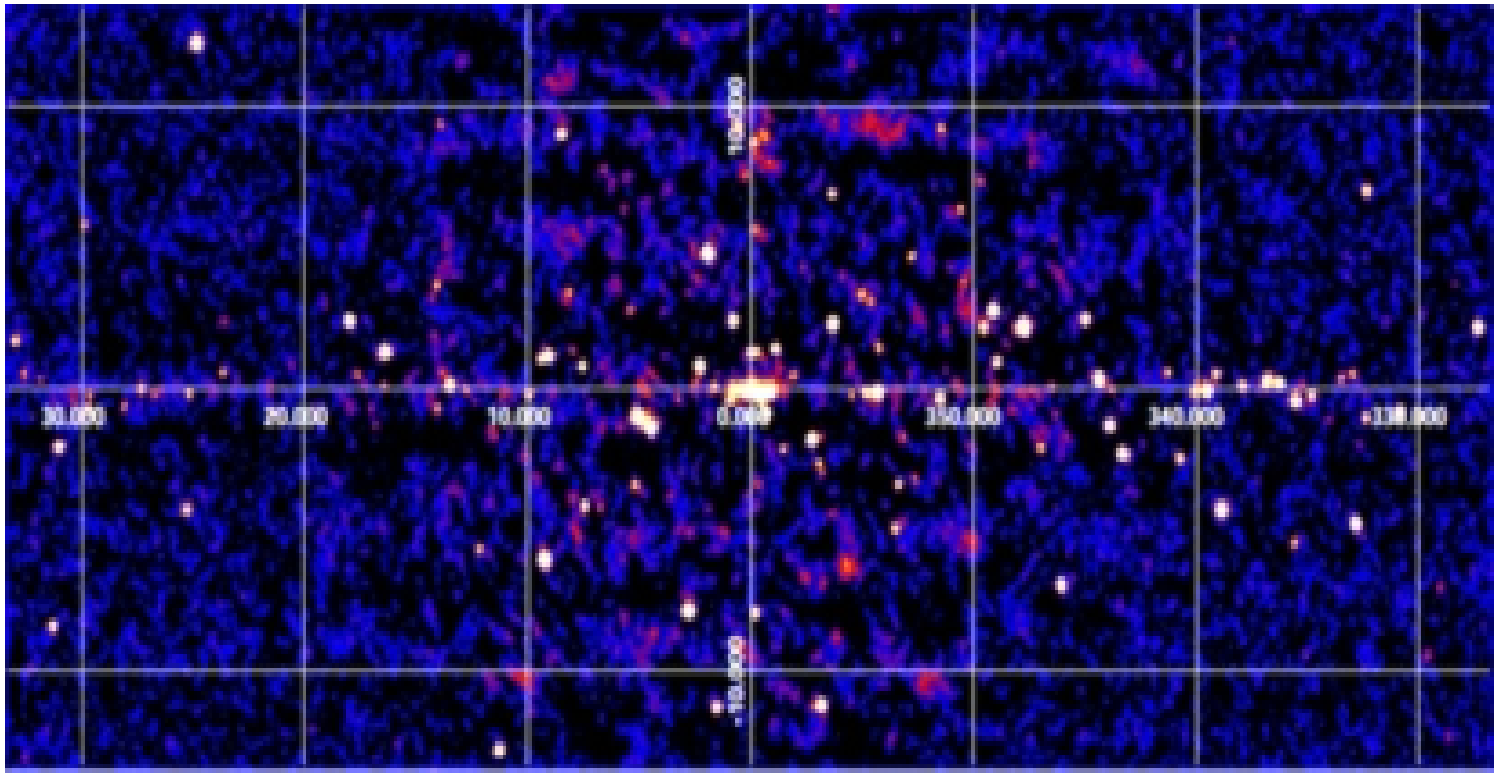

INTEGRAL, 20 Msec, 17-60 keV,

Agata Różańska, fall semester, 2022/23

CHANDRA and JWT – Cartwheels galaxy

HEASARC
Picture of the Week

APOD: Astronomy Picture of the Day

More Images

The principle mode of measurement in X-ray astronomy is to detect individual photons to determine the set of four properties:

1) arrival direction
2) energy of the photon
3) time of arrival of the photon
4) its polarization angle

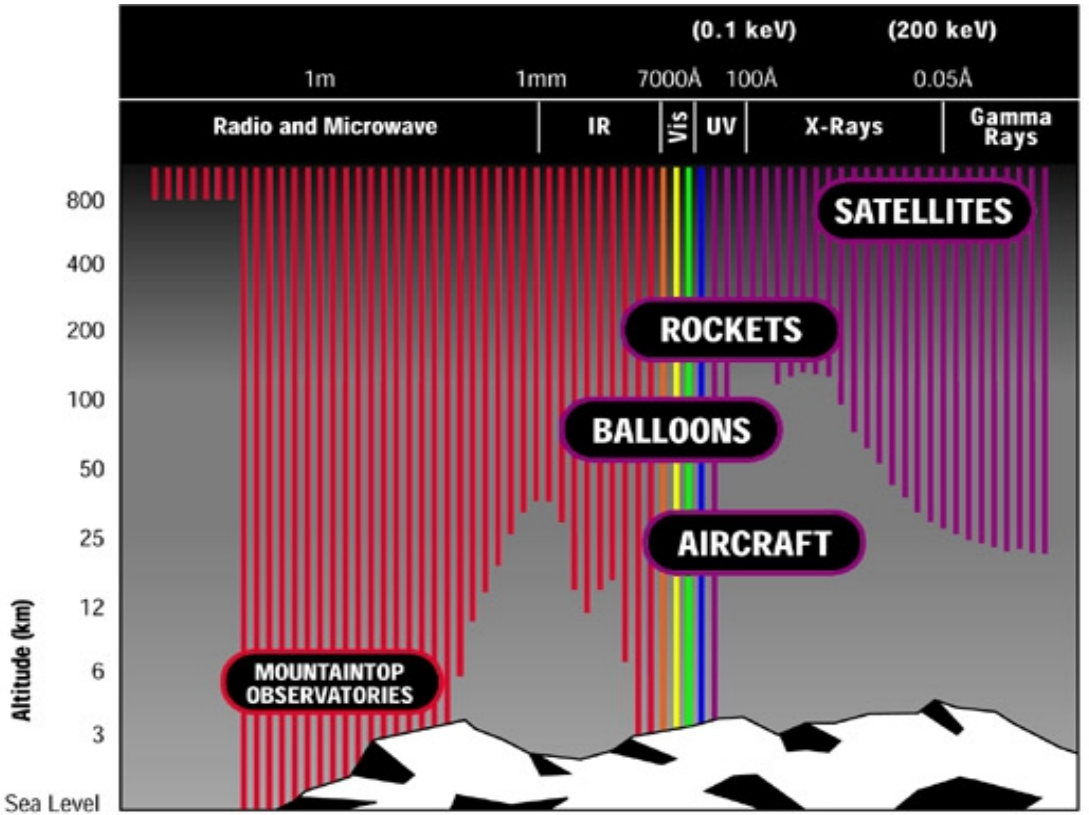

Short history of the X-ray astronomy:

1946 – Herbert Friedman from Naval Research Laboratory had put up Geiger-Müller's proportional counter on the V2 rocket. They have observed weak emission from Solar corona (1948).

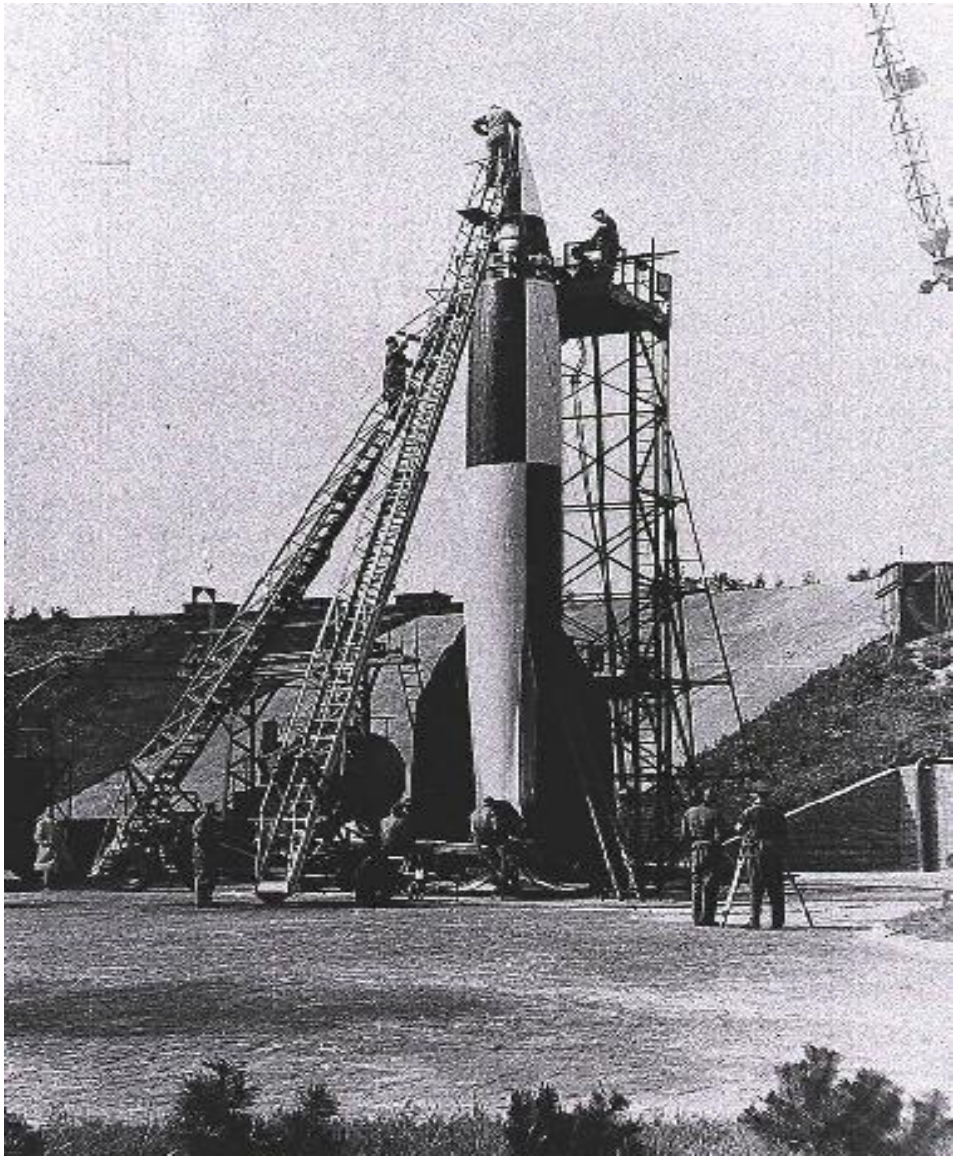

AEROBEE rocket 1909

Aerojet General 1946,
first instrument
was lunched 1948.

1951 – Hans Wolter
has prooved,
that X-rays can be
focused, by hiperbolic
or parabolic mirrors –
Wolter Mirrors.

Grazing incident
Mirror systems as
imaging optics
for X-rays, 1952
Ann. Physik, 10, 94.

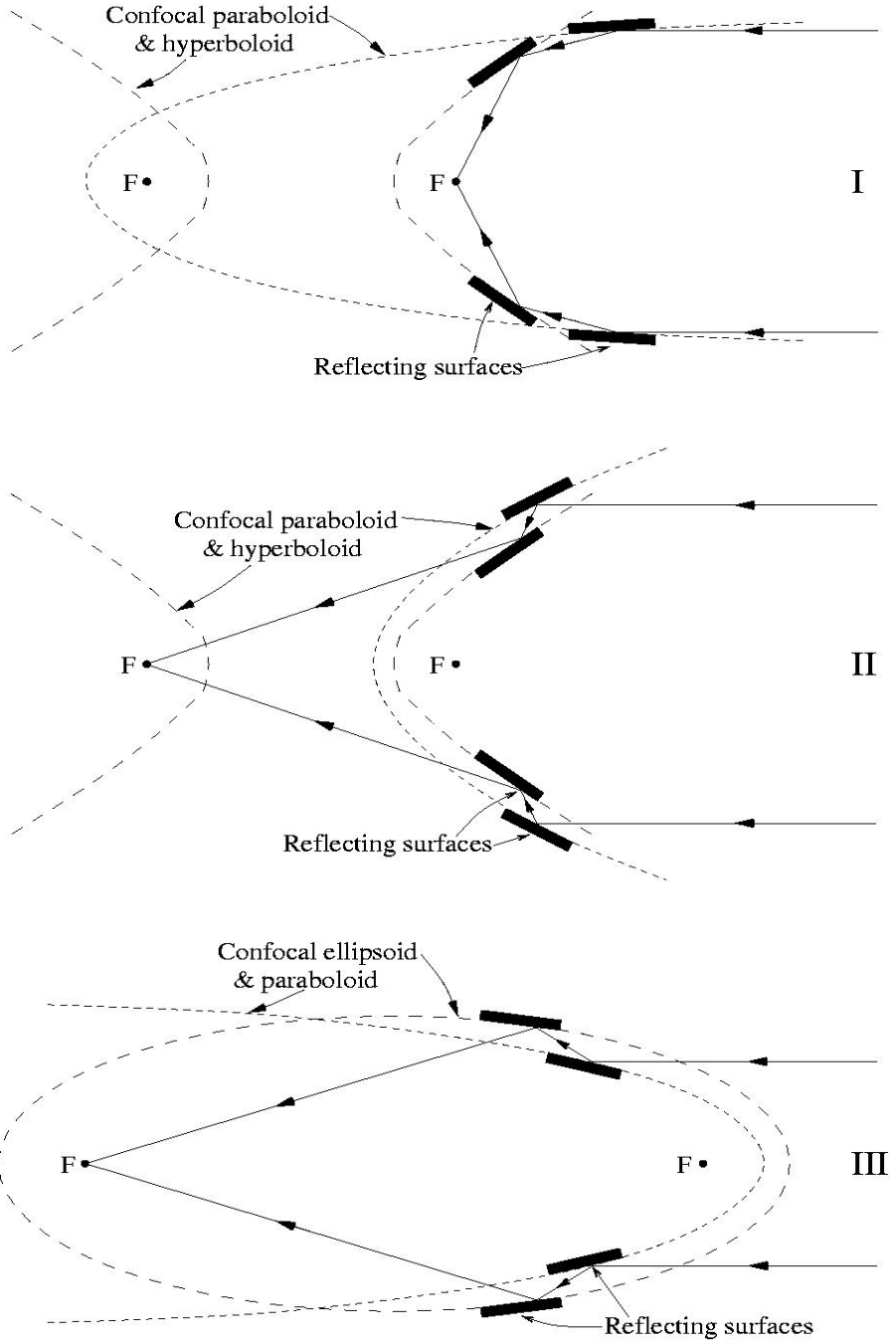

1962 – Riccardo Giacconi
from American Science
and Engineering Cambridge,
had put up proportional
counter (2-10 keV)
on AEROBEE rocket.
He discovered
Scorpius X-1,
and diffused X-rays
from all directions.

2002 Nobel Prize Winner.

Physical Review Letters, Dec. 1st, 1962, Vol. 9, pp 439,
"Evidence for X-Ray From Sources Outside the Solar System".

1963 – Riccardo Giacconi with collaborators have made the first X-ray image of the Sun using small Wolter telescope on the board of rocket.

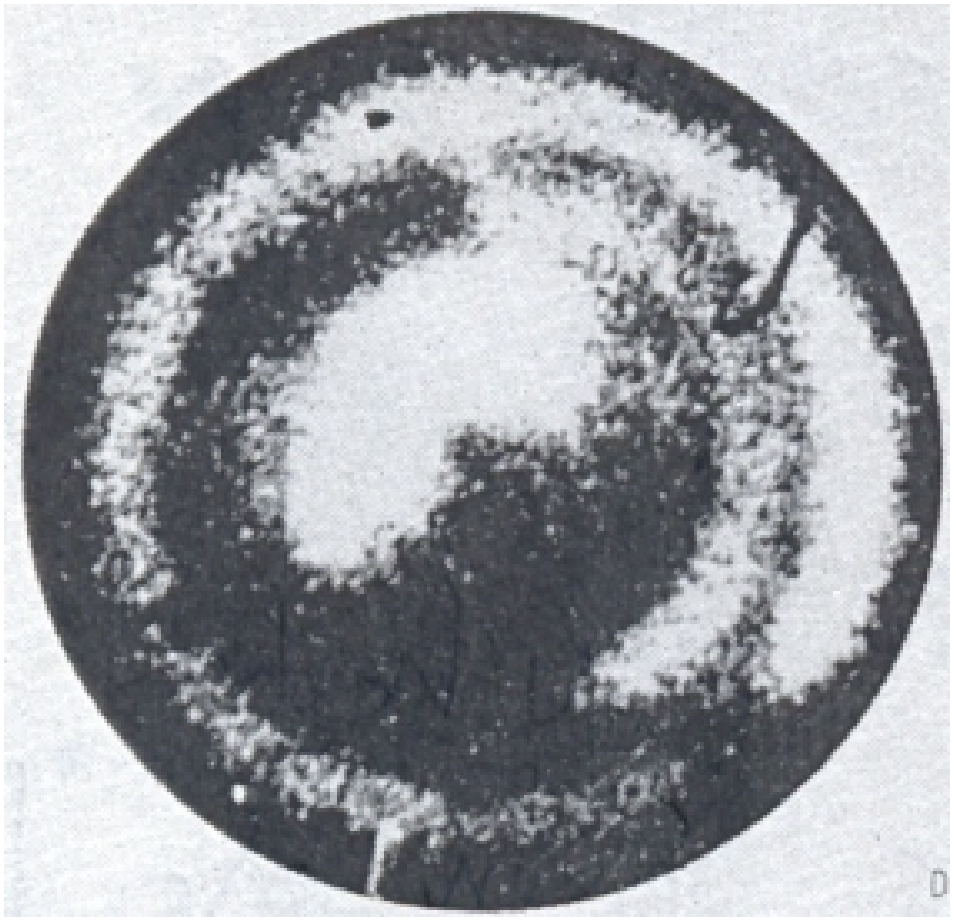

1963 – Riccardo Giacconi with collaborators have made the first X-ray image of the Sun using small Wolter telescope on the board of rocket.

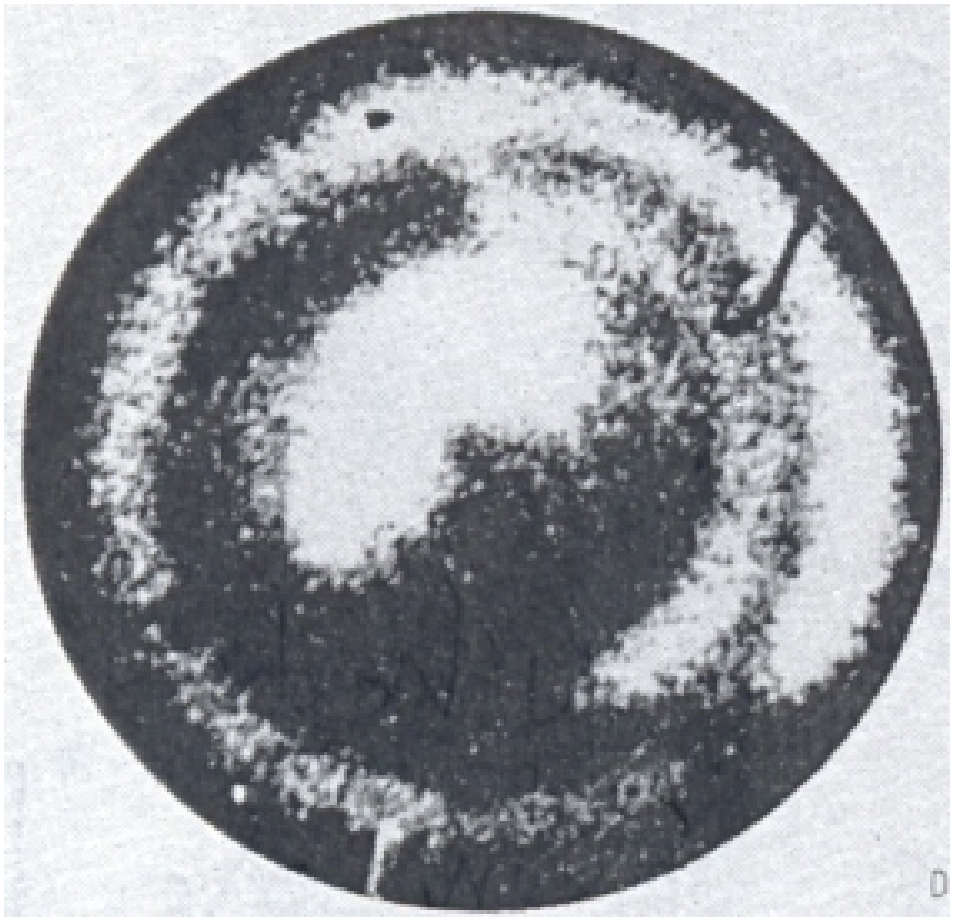

NuSTAR hard X-rays – blue

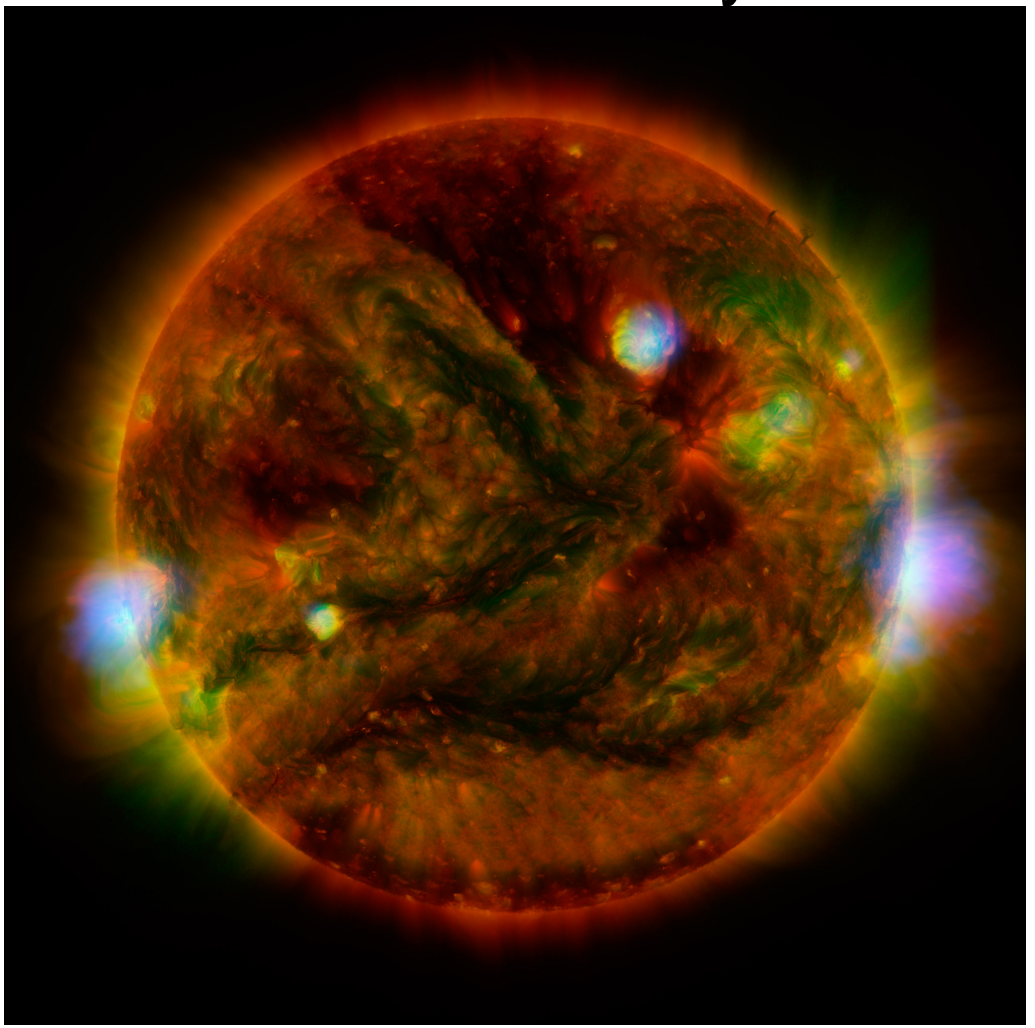

1970-1981 – **UHURU, VELA, SKYLAB, HEAO-1, EINSTEIN.**
Cristal spectrometers and the first mirror on large telescope. Clusters of galaxies, warm gas, AGN, X-ray binaries, X-ray background.

1983-2000 – **EXOSAT, ROSAT, ASCA, BEPPO-SAX.**
Quasi-periodic oscillations, Timing, X-ray bursts and outbursts, all sky survey.

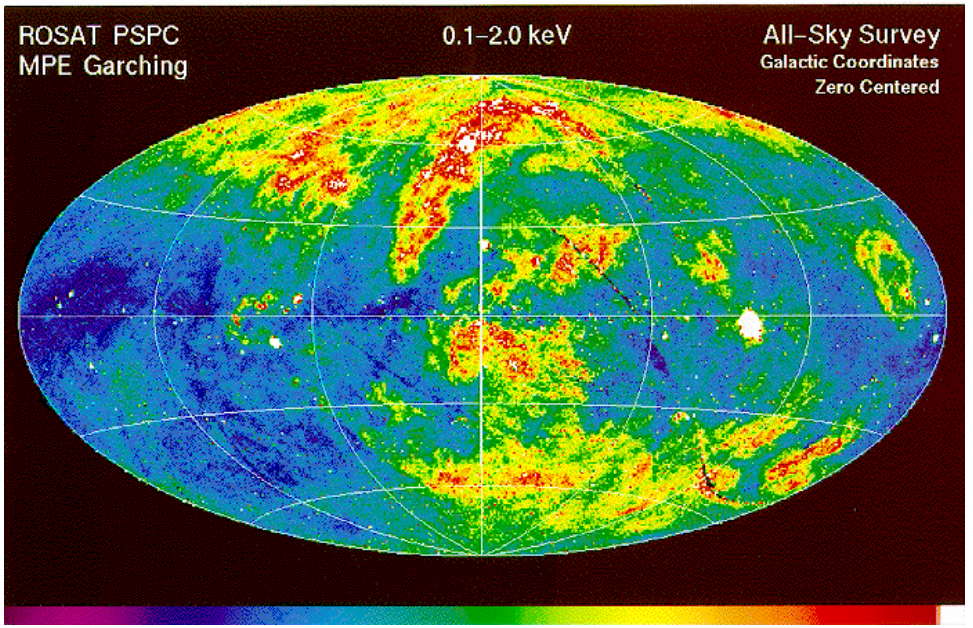

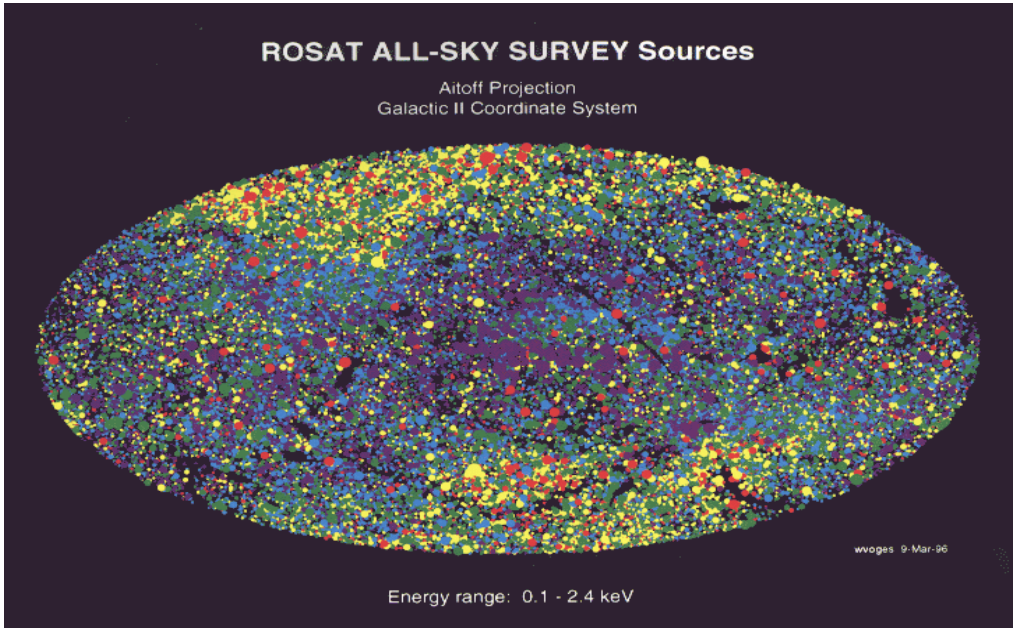

The 2020 All-Sky Survey by eROSITA – now in off mode

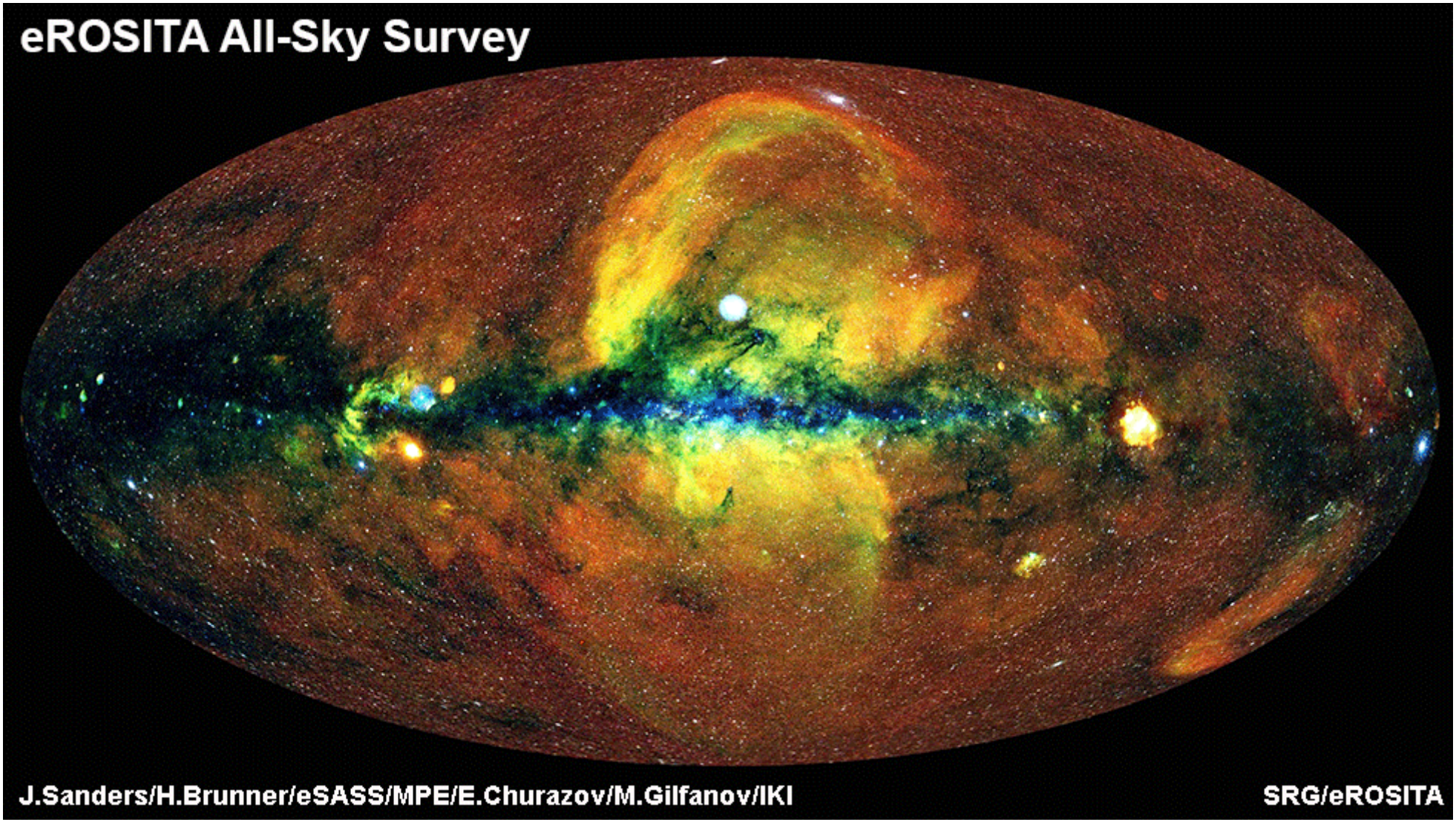

Currently working satellites:

1999 – CHANDRA, 0.1-10 keV, high resolution camera, transmitting gratings.

Great imaging of 1 arcsec resolution.

X-ray Jet, PKS 1127-145

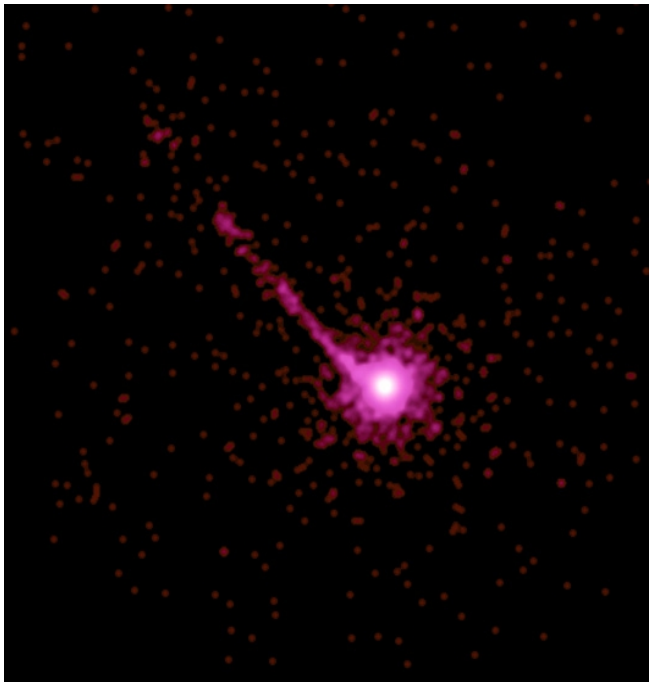

Crab Nebula

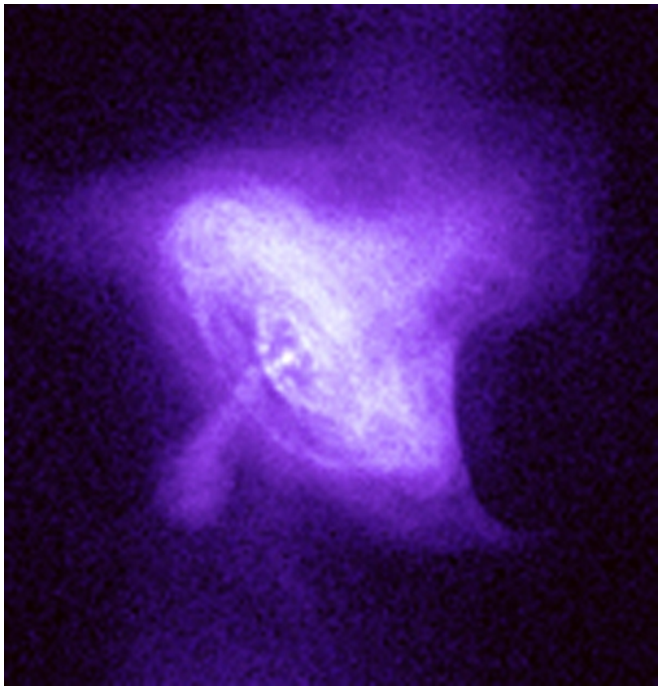

Vela Pulsar

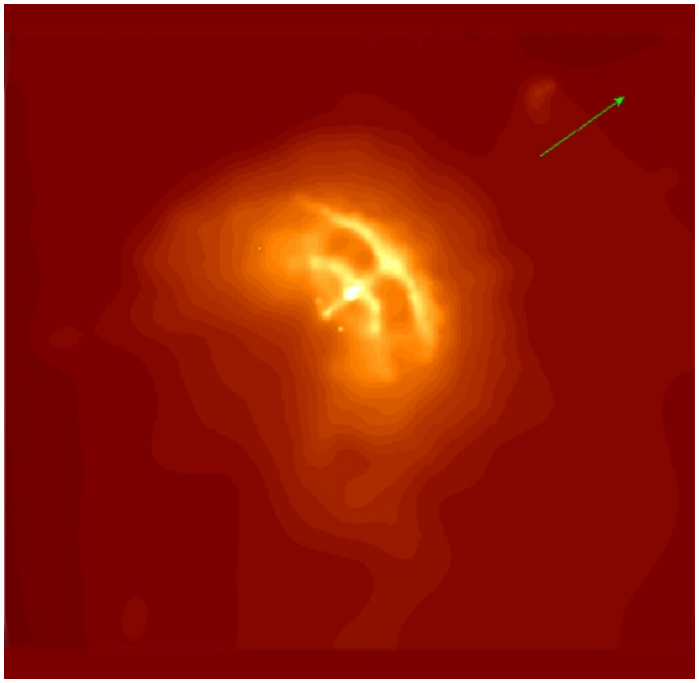

Milky Way with CHANDRA
X-ray telescope

CHANDRA X-ray spectroscopy

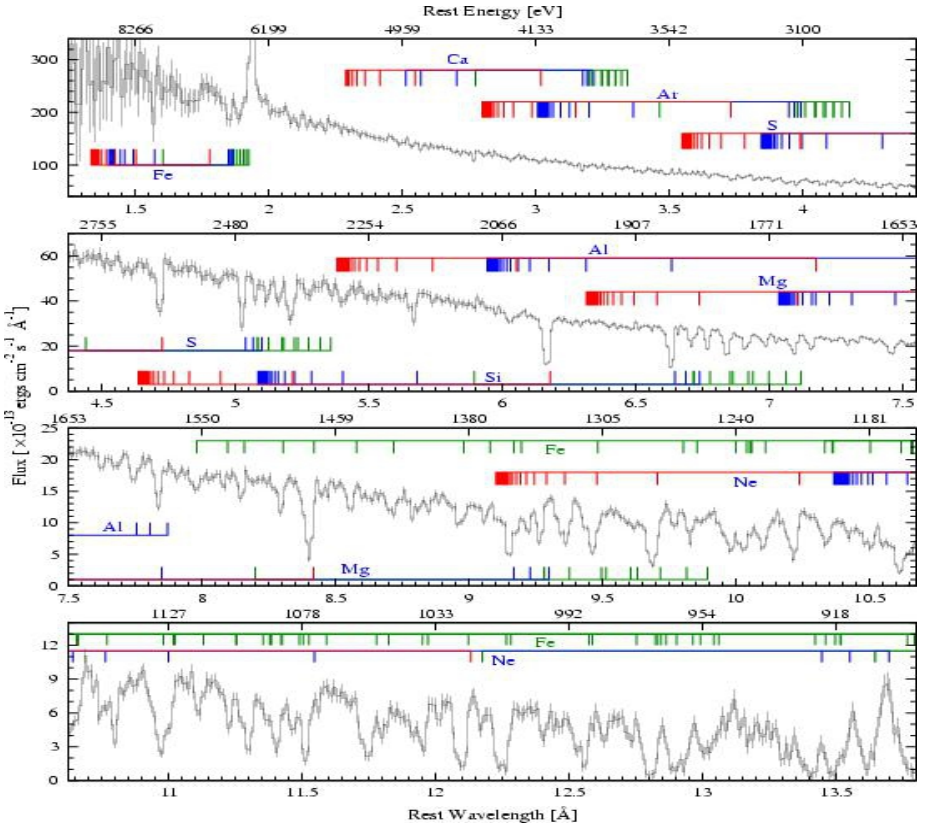

Kaspi et al. 2002, 900 ksec.

Cottam et al. 2002 Nature
z=0.35

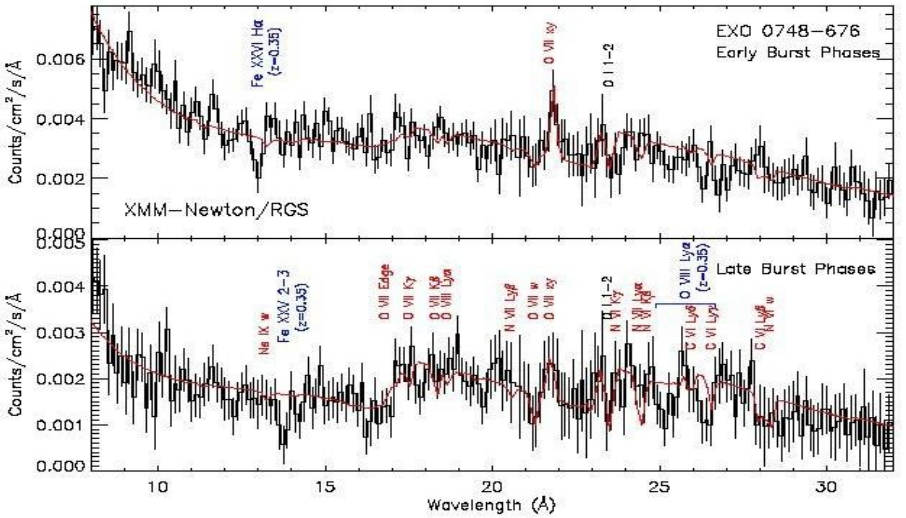

X-ray burst spectra of a neutron star

Image courtesy of J. Cottam, NASA GSFC

1999 – XMM-NEWTON,
0.2-12 keV,
reflecting gratings,
gravitational redshift,

HITOMI – mission with micro-calorimeter, JAXA - 2016

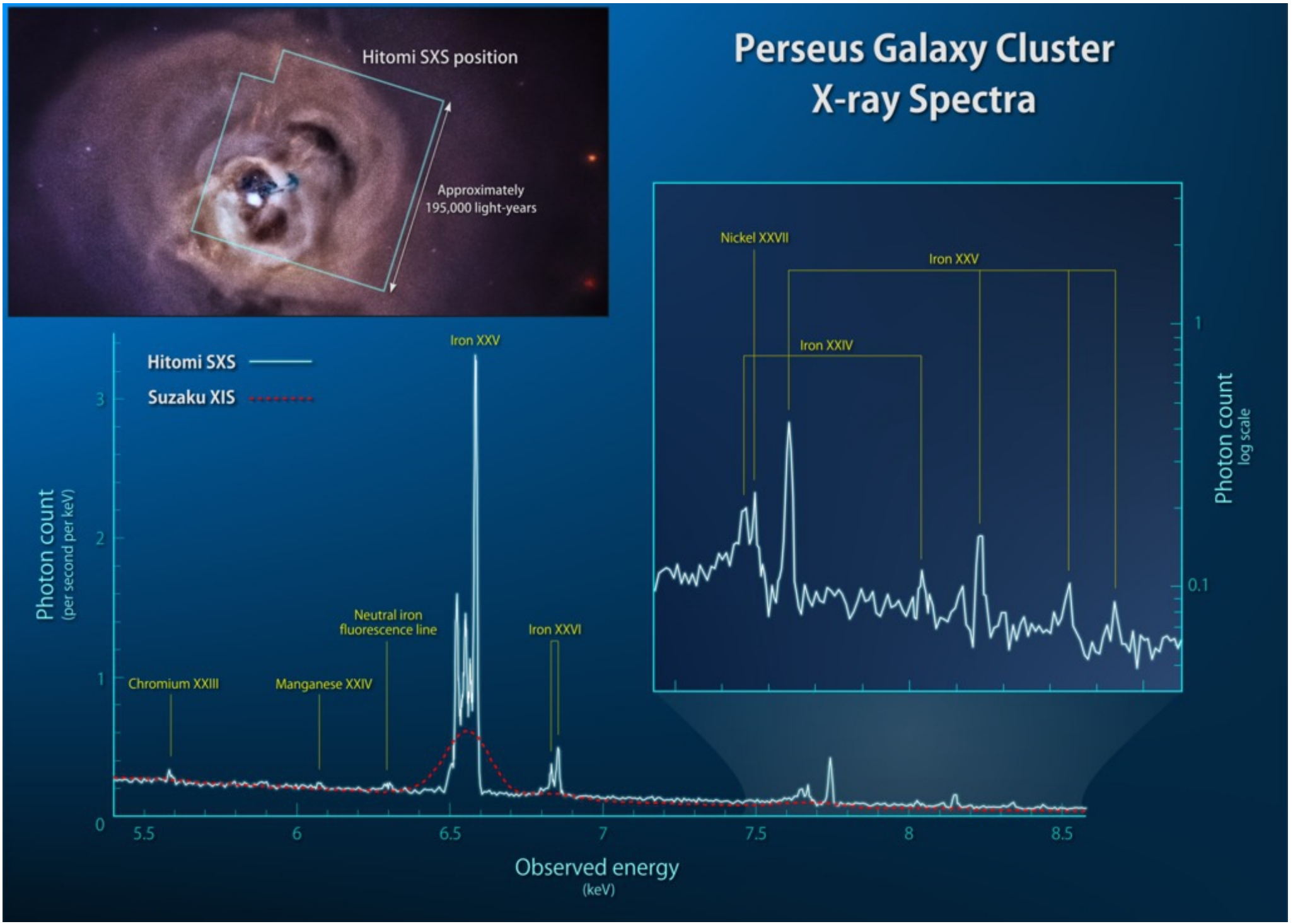

MaGIXS (NASA mission 2021), **CORONAS-F**, **Yonkoh**,

2002 – **INTEGRAL**,
15 keV- 10 MeV,
GRB, timing and
broad-band spectra

18 keV-8 MeV light curve
7 sec. grouping,
Borkowski et al. 2004

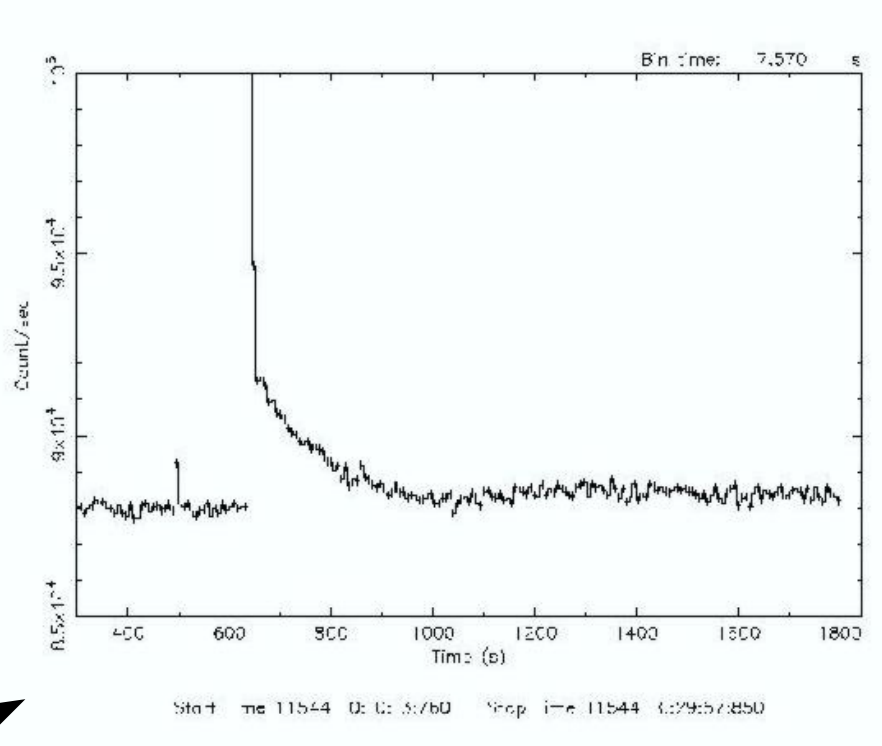

2004 – **SWIFT**, 0.2-150 keV, up to 200 GeV,
UV, optical band, GRB, broad-band spectra

MAXI, FERMI, AGILE, NICXER, IXPE

IXPE – NASA mission launched on 2021,
NICER – JAXA mission launched on 2017

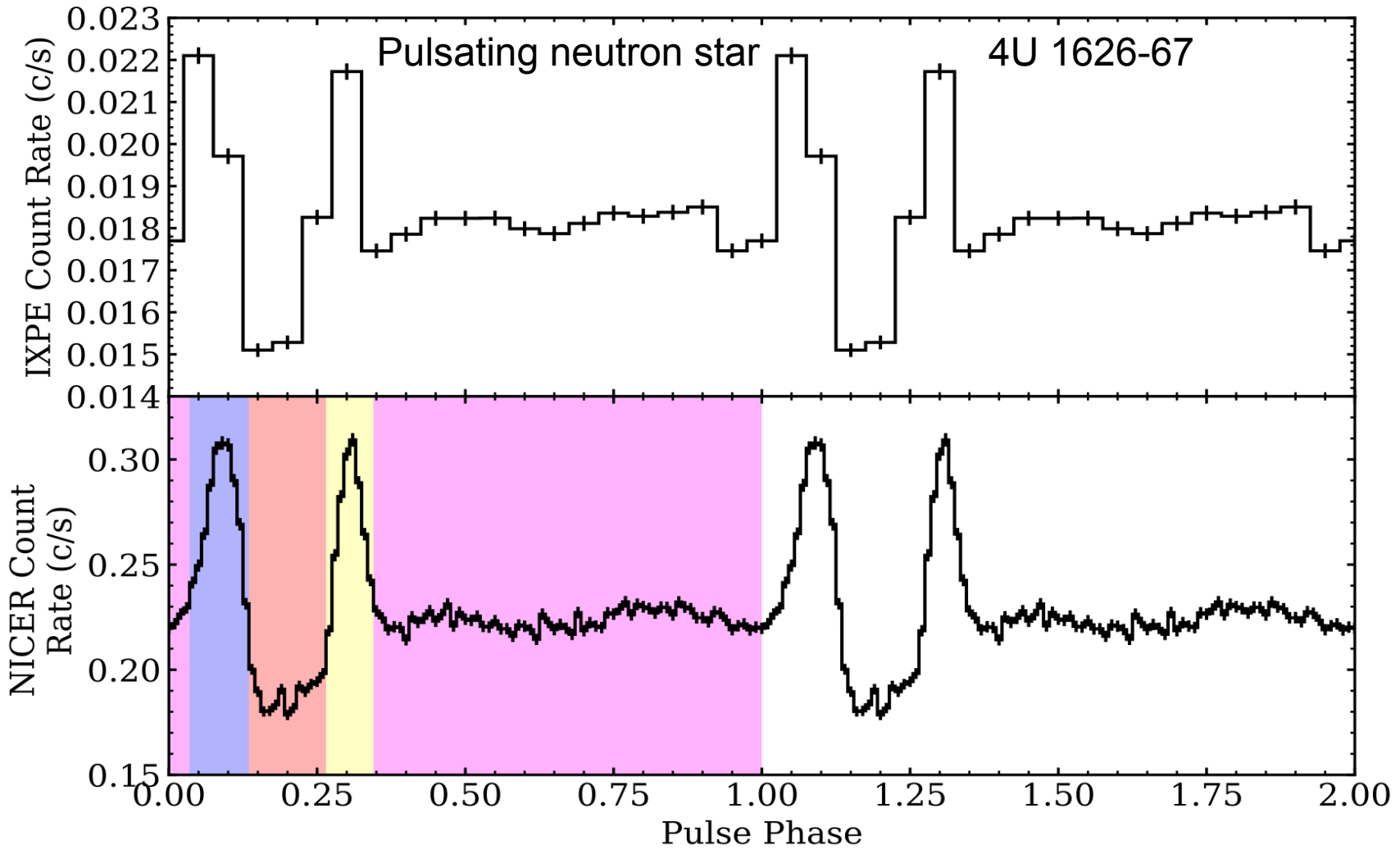

Figure 4. Top: Folded 2.0–8.0 keV pulse profile for 4U 1626−67 with the combined IXPE events from all three detectors. Bottom: Folded 2.0–8.0 keV pulse profile for 4U 1626−67 using NICER data. The two peaks correspond to pulse phase values 0.0907 and 0.3076 (derived from fitting a parabola around the peaks). The different colors represent the pulse phase intervals used in the analysis of Sect. 3.3: a) 0.345–0.035 (modulo 1; pink), b) 0.035–0.135 (blue), c) 0.135–0.265 (red), and 0.265–0.345 (yellow). The phase boundaries were based on the structure of the NICER pulse profile. The pulse profiles are phase-aligned and two rotation cycles are plotted for clarity.

Part 1. **TELESCOPES**

Part 2. **OBSERVATIONS**

Part 3. **THEORY**

Lecture 1: Proportional Counters- PC

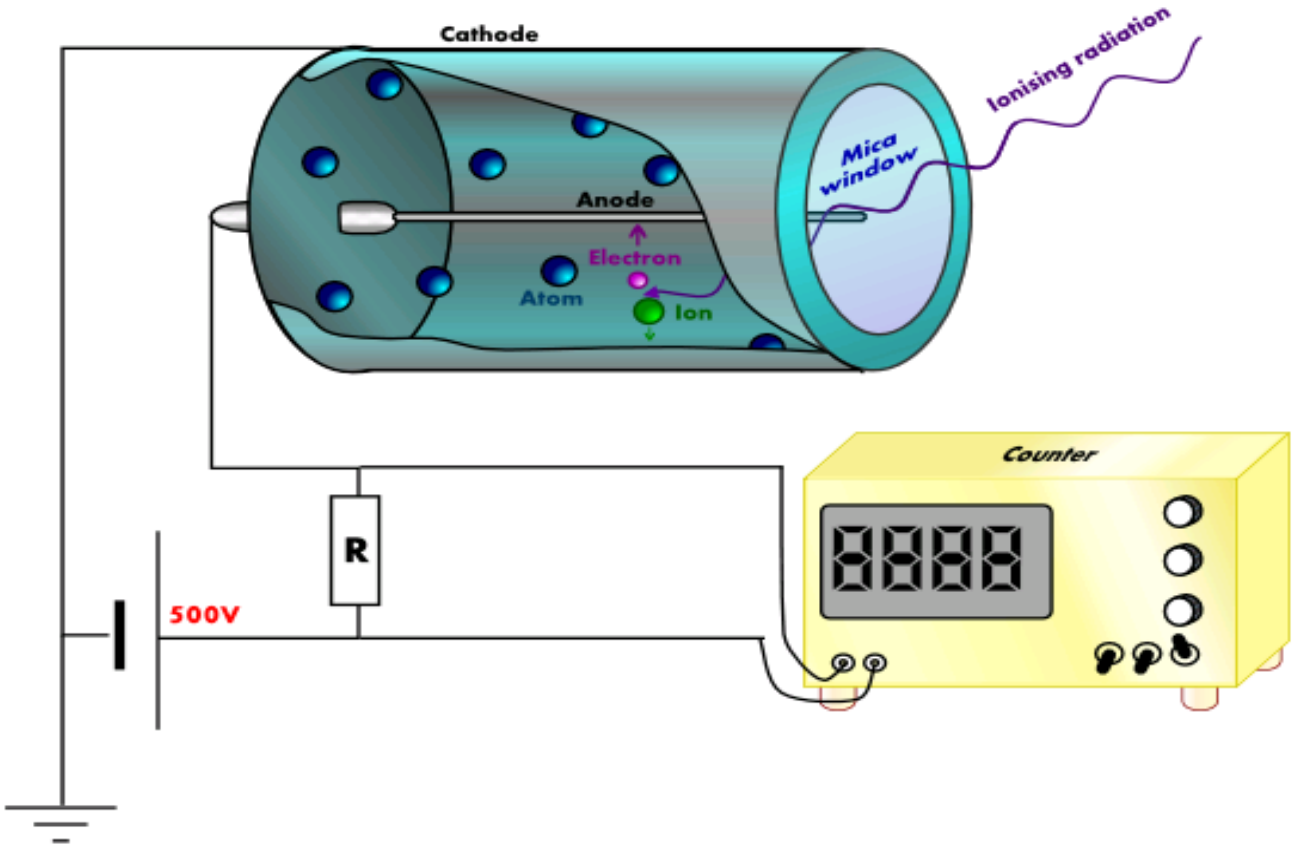

Gaseous detectors operate in different modes depending on the type of gas and on the electric field strength in the capacitor.

Electric field strength in capacitor :

- ionization chamber mode
- gas scintillation proportional counter – UV radiation
- collisions and charge multiplication takes place, as far as it is proportional to the original number of electrons- PC
- avalanche propagates through the whole detector – Geiger Mueller mode,
- the spark chamber mode at the highest field strength.

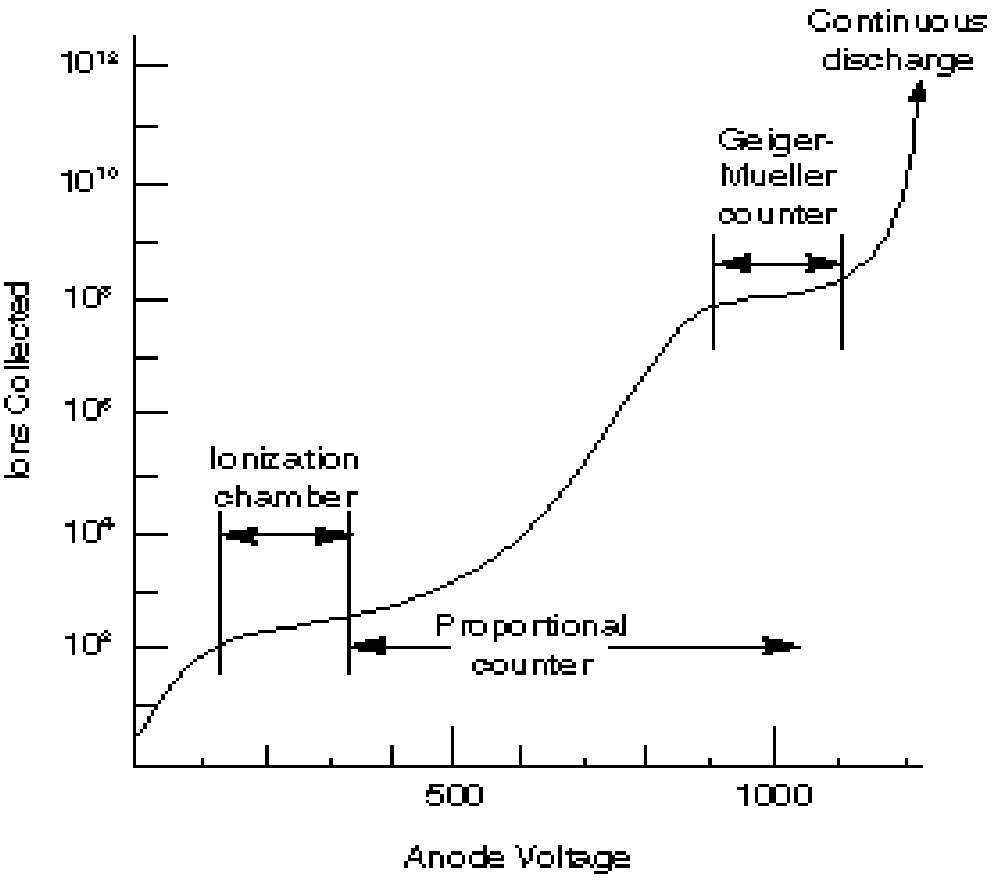

The photo effect cross section scales as:

$$\sim Z^n E^{-\frac{8}{3}}$$

where E is the X-ray energy, Z is the atomic number of the gas, n≈ 4-5.

The number of pairs electron-ion generated by this event is:

$$N = E / W$$

where W is the average energy for the creation.
W depends on the detector noble gas:
usually 20- 30 eV.

A 1 keV X-ray photon creates 30-40 electron-ion pairs.....

Electrical field strength is a function of radial distance, r, from the tube center (anode):

$$dU/dr = U_o/[r(\ln r_c/r_a)]$$

anode wire voltage

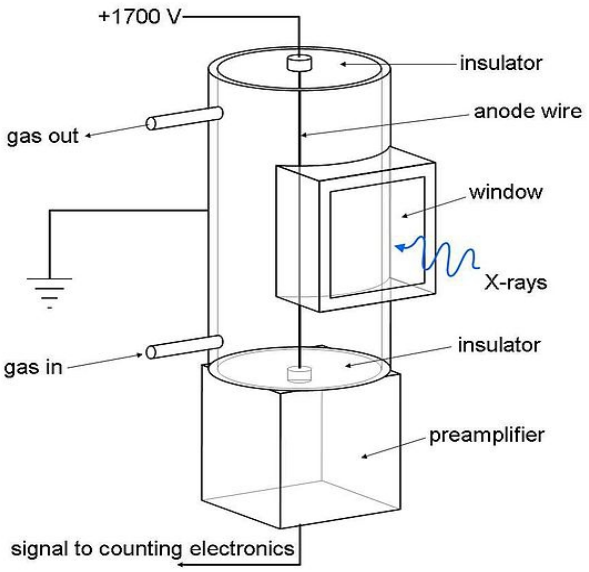

Electrons – small fraction of output signal with a short rise time.

Ions – the main portion of signal with a rise time of 100 μs.

Additional events: - generation of UV photons, by excitation of gas atoms , and neutralization of ions on arrival at the cathode,
- UV induce the emission of electrons.

Quench gases: – (few %) absorb UV and convert them via radiationless transitions into heat.

Quantum Efficiency of PC:

1) – transmission on the thin window
2) – absorption of the detector gas

$$Q = T\, e^{-d\,\kappa_w}\left(1 - e^{-h\,\kappa_g}\right)$$

κ_w - energy dependent transmission coefficient for wind,
d - window column density in g cm^{-2},
κ_g - energy dependent absorption coefficient for gas,
h - gas column density in g cm^{-2}.

metallic window – beryllium 25μm, alluminium > 1.5 keV,
plastic window – polypropalene 1μm, down to 0.1 keV

noble gas with 5-20 % of quench gas, κ_g depends on Z

for law energies – argon
for high energies – xeon

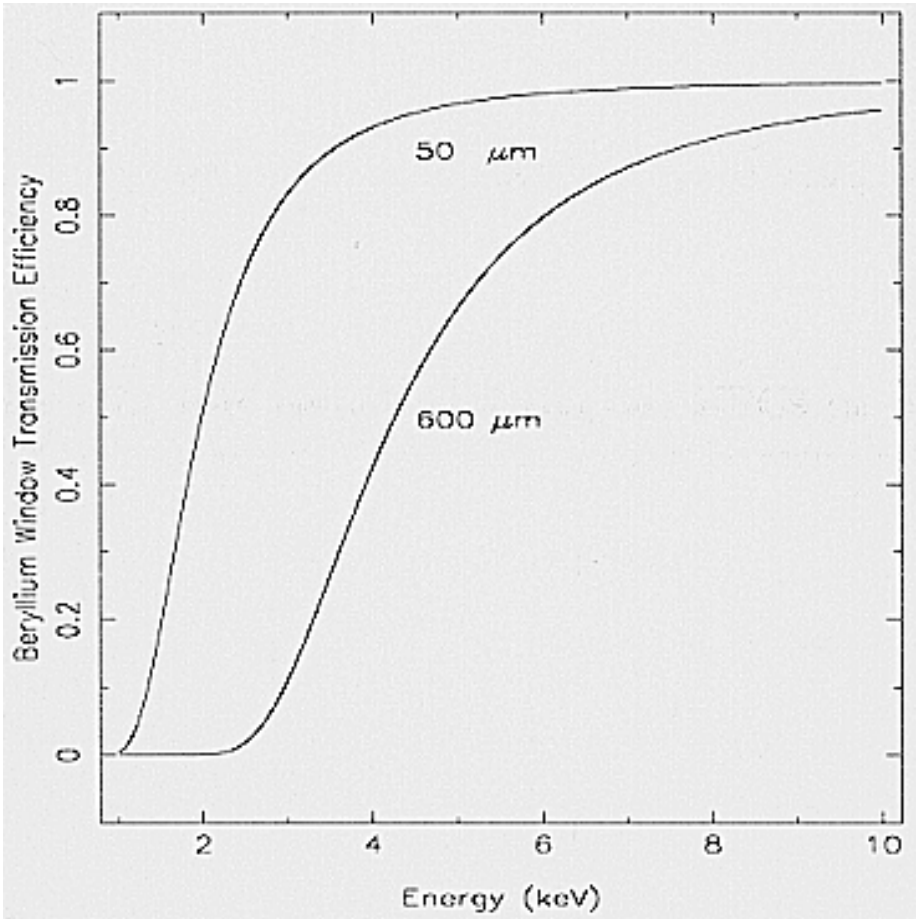

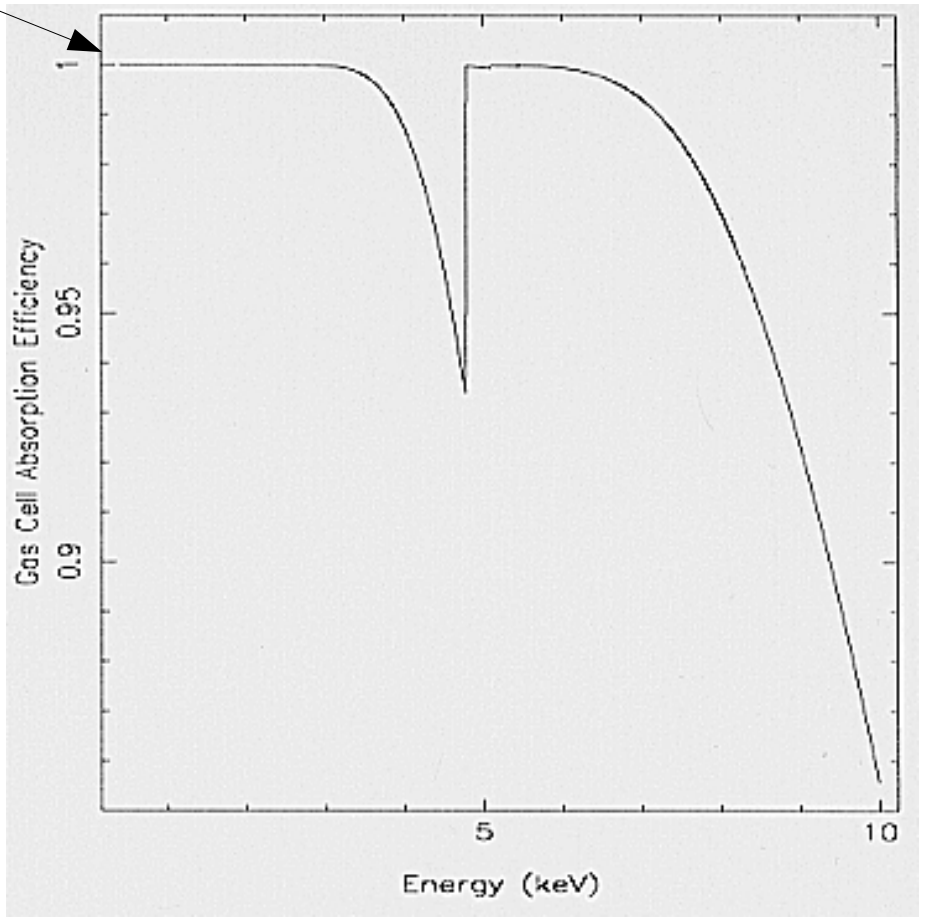

PCs have moderate Energy Resolution:

determined by statistic of initial ionization process:

$$\left(\frac{\sigma_N}{N}\right)^2 = \frac{F}{N}$$

Fano factor is an empirical constant ≈ 0.05-0.2,

variance of the number N of electron-ion pairs created is less than Poisson statistics, because collisions of the ionization process are not statistically independent,

and by the statistic of charge multiplication:

$$\left(\frac{\sigma_A}{\bar{A}}\right)^2 \approx b$$

variance of the amplification A of a single electron b ≈ 0.5-0.6

$$\left(\frac{\sigma_E}{E}\right)^2 = \left(\frac{\sigma_N}{N}\right)^2 + \frac{1}{N}\left(\frac{\sigma_A}{\bar{A}}\right)^2 ; \qquad \frac{\sigma_E}{E} = \sqrt{\frac{F+b}{N}}$$

PCs time resolution:

High drift velocity of electrons in gases 10^6-10^7 cm s^{-1}, so time resolution below 1μs can be achieved.

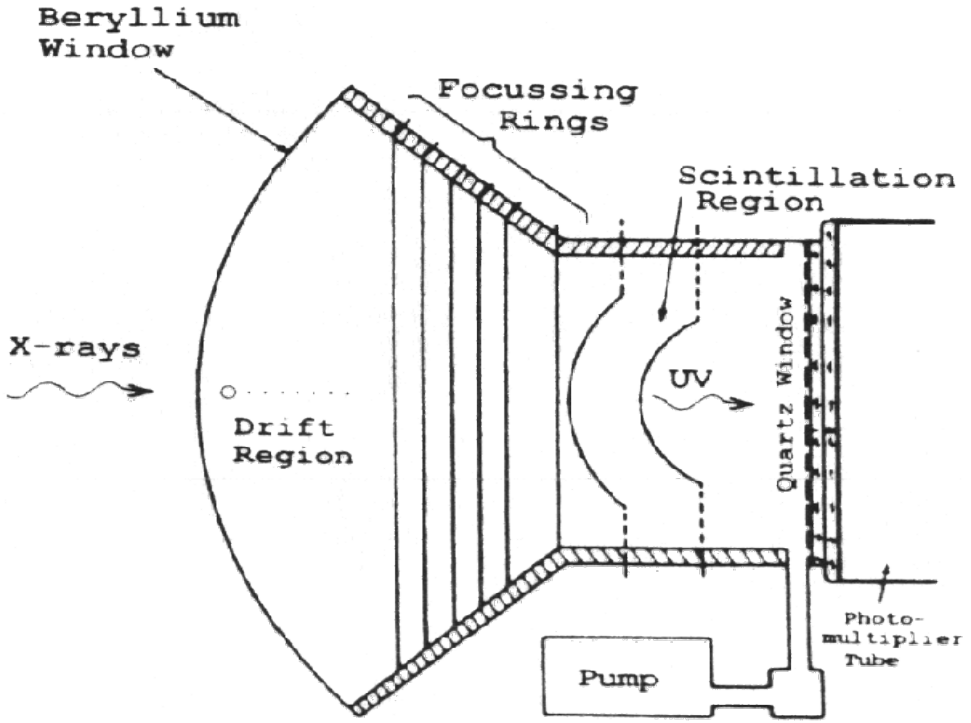

Drift region – between absorption position of the X-rays and the avalanche or scintillation region.

Background Rejection Capability: important !!!

the background rate exceeds by far the X-ray event rate for the majority of cosmic X-ray sources....

cosmic rays - charged particle events,
fluorescent X-rays from surrounding materials.

Sophisticated event selected logic is mandatory.....

limit the energy band of accepted events – the depth of the detector cell must be large enough so that minimum ionizing particles deposit more energy than the most energetic accepted X-ray event,
geometrical shape of the related ionization cloud,
the gas column density should be large to absorb bad X-rays.

X-ray detector surrounded with anticoincidence detectors
-signal detected by both should be rejected,

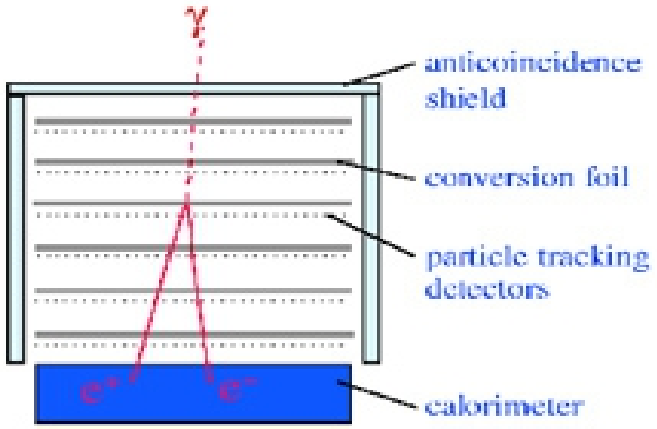

The HXD background

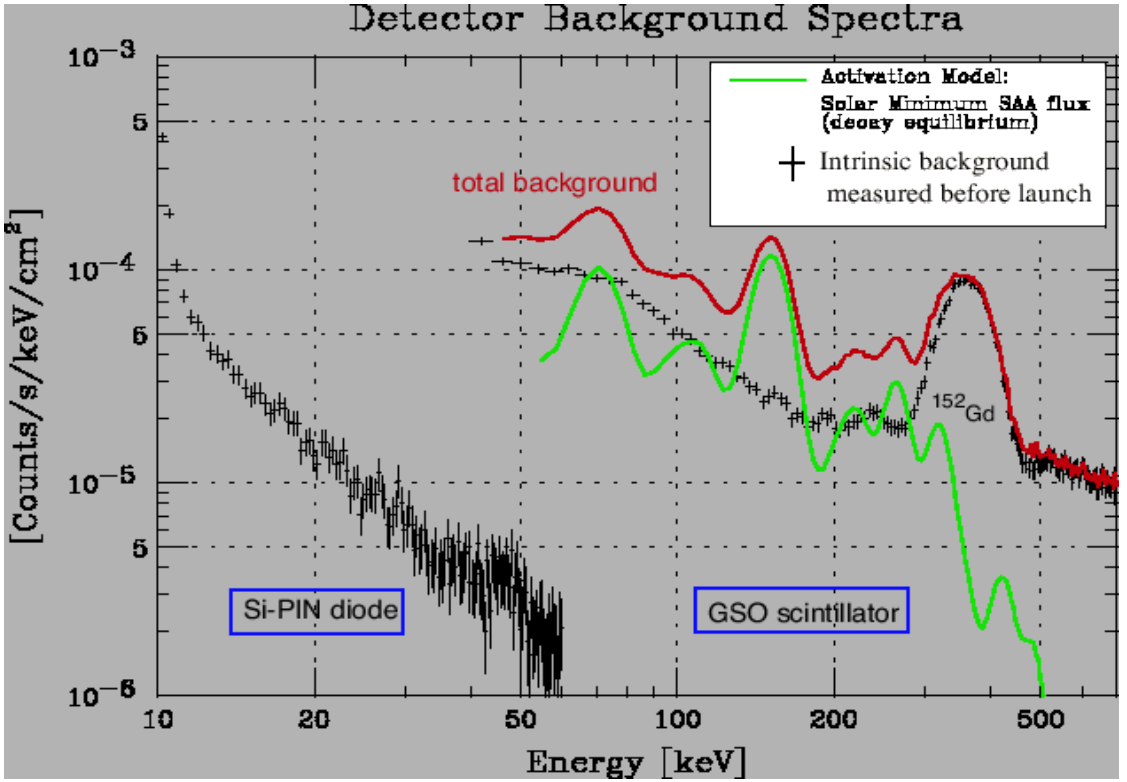

Detector's lifetime:

The radiation environment can damage a PC in two ways:

1) Heavy ionizing particles can deposit energies 3-4 orders of magnitude higher than X-rays:
   -it can trigger a permanent discharge
   -or destroy the detector by spark discharge.

2) Cracking of the quench gas molecules during normal operation:
   - CH_4 tends to deposit polymerization products on anode and cathode wires – Malter effect.

Gas purity, composition, wire, housing materials, el. field contribute to the radiation dose tolerated by the detector.

Non-imaging instruments require LARGE AREA detectors with high background rejection capability. E up to 50 keV.

RXTE $A_{coll} = 6250\ cm^2$

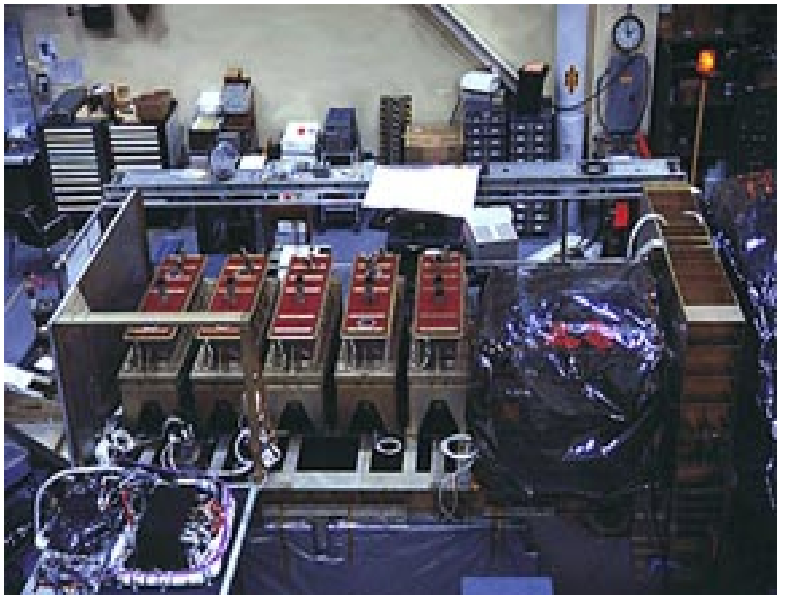

GINGA $A_{coll} = 4000\ cm^2$

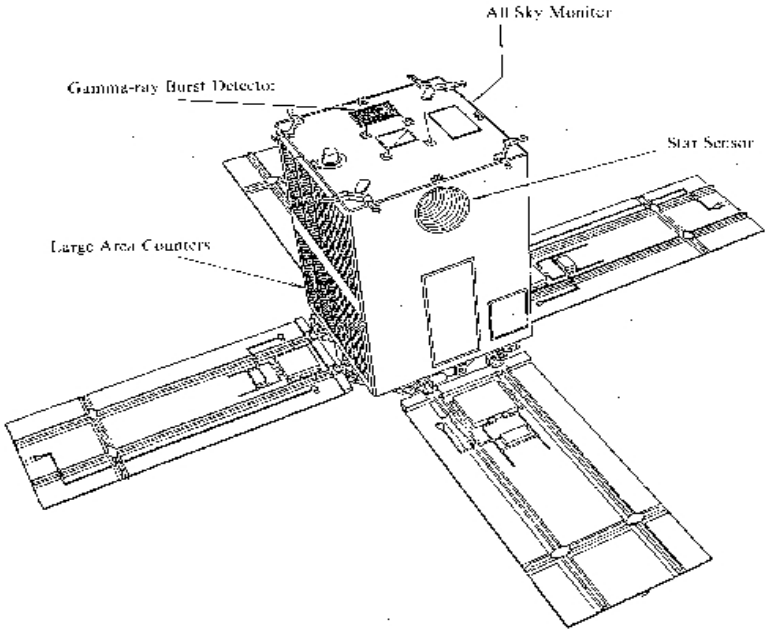

Fig. 1. The LAC instrument showing the eight coaligned collimated proportional counters mounted on the Y face of the spacecraft.

The cell structure of those detectors offers different possibilities for discriminating background events....

LARGE AREA PC's detection limit for a point source:

Q - quantum efficiency of the detector

A_X – geometric detector area for X-rays (cm^2)

A_b – geometric detector area for background (cm^2)

B_c – cosmic-ray bkg event not rejected (event/cm^2/s/keV)

B_x – diffuse cosmic X-ray bkg (event/cm^2/s/keV)

Ω - field of view (sr)

F_{min} – min. detectable flux of point source (ph/cm^2/s/keV)

ΔE – energy band of the detector (keV)

S – desired number of standard deviations

t – observing time (s)

$$F_{min} = \frac{S}{Q A_x} \sqrt{\frac{B_c A_b + Q \Omega B_x A_x}{t \Delta E}}$$

Gas Scintillation Proportional Counters, GSPC:

GSPC – X-rays are absorbed by the detector noble gas in the absorption drift region.

Charge released, by an ionizing event is not amplified.

Electrons drift into the scintillation region, where they acquire sufficient energy to excite gas by collisions.

The number of UV photons increases linearly with the number of collisions.

UV photons in the range of 150-195 nm (for xeon gas).

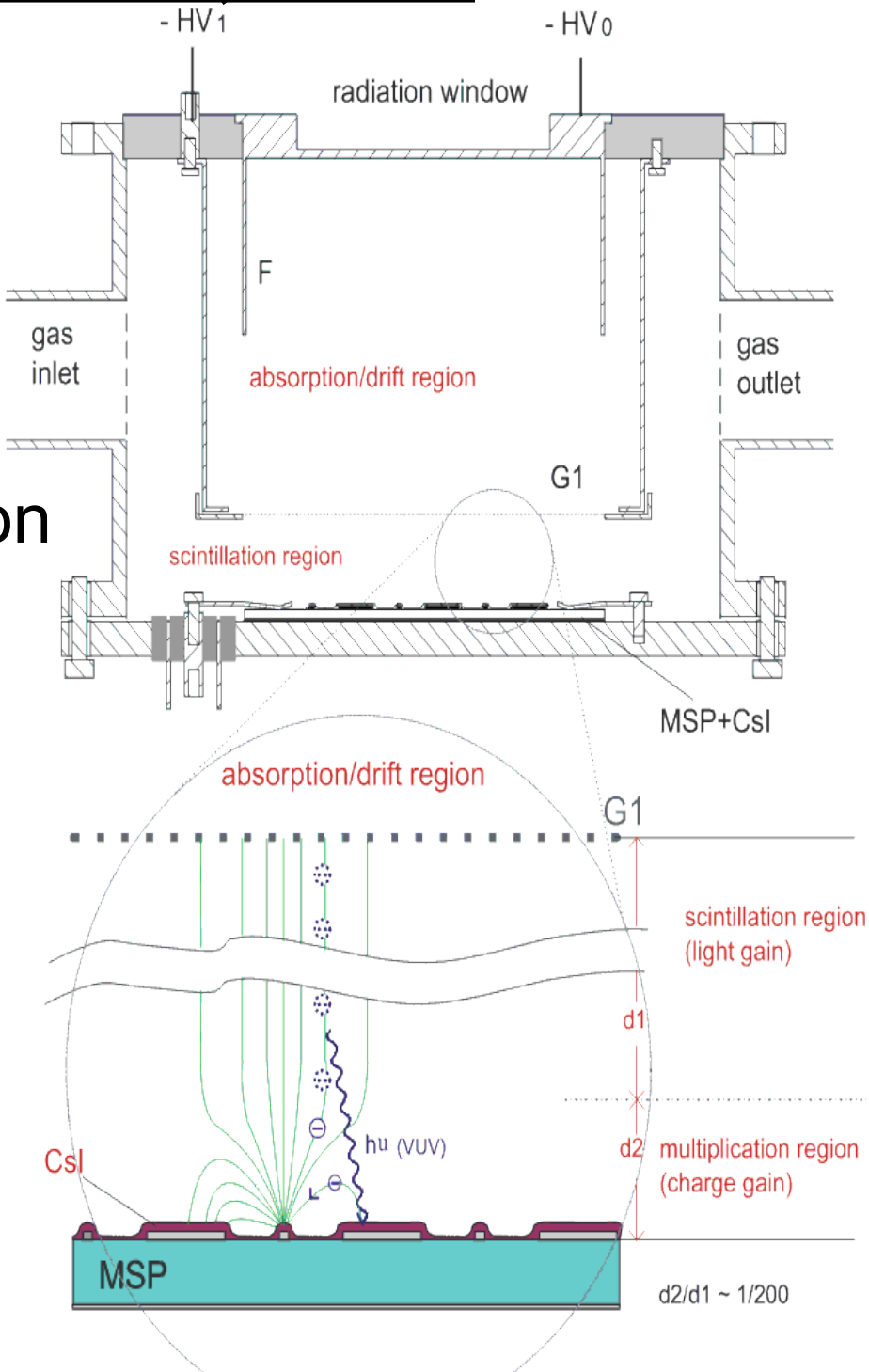

Fano number limits energy resolution of PC by almost a factor of two. About 14 ionizing collisions result in charge multiplication of four orders of magnitude.

In case of GSPC, the variation of the light output generated during the scintillation process depends on the statistics of the final number of photons registered by the photomultiplier. The integral intensity of the light flash is proportional to the energy of the ionizing event.

GSPCs can reach an energy resolution nearly the Fano limit because of the large amount of scintillation photons.

They are sensitive to the purity of the gas... !!!!!!

Scintillation Counters:

Hard X-ray Detectors > 15 – 100 now-days: 400 keV

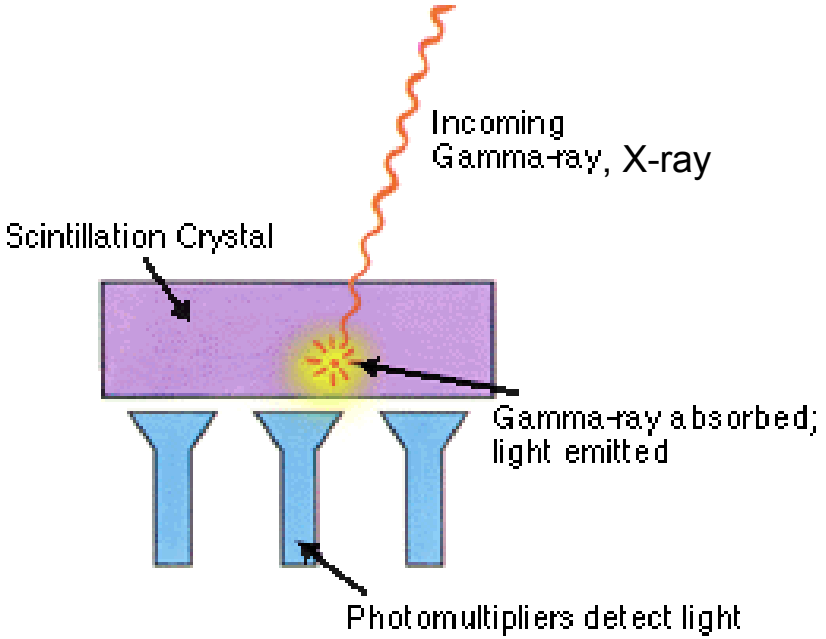

Inorganic scintillating crystals optically coupled to a phototube or photodiode. Incident radiation energy is converted into optical photons and measured as an electric pulse by the light sensor.

Ideal scintillation material (crystals):

- High linear scintillation efficiency,
- Transparency to its own light (light yield),
- Emission spectrum should fit to the spectral response function of the light sensor,
- High photon absorption cross section,
- Decay time of the induce luminescence should be short.

Material	Light Output (photons/Mev)	Wavelength of Max. Emission (nm)	Decay Constant (nsec)	Density gms/cc	Index of Refraction	Moisture Sensitivity	Afterglow % of Signal After (___) msec
NaI(Tl)	38,000	415	230	3.67	1.85	High	0.3-5 / 6msec
BGO	9,000	480	300	7.13	2.15	None	0.005 / 3msec
CsI(Tl)	59,000	560	1000	4.51	1.84	Slight	0.5-5 / 6msec
$CdWO_4$	15,000	480	1100/14500	8.00	2.20	None	0.1 / 3msec
CaF_2(Eu)	19,000	435	940	3.19	1.44	None	<0.3 / 6msec
GOS*		510	3000	7.34	2.20	None	<0.1 / 3msec
LSO**	30,000	420	40	7.40	1.82	None	
Plastics	~10,000	420	2-17	1.03	1.58	None	<0.1 / 3msec

* Gd_2O_2S with dopants; properties vary with dopant types and levels.[2]

** $Lu_2(SiO_4)O$:Ce

Basic operating principle

X-ray/gamma-ray absorber - e.g. CsI, NaI, BGO

Light guide

Light -> e^- converter (PMT/diode)

Electronic signal

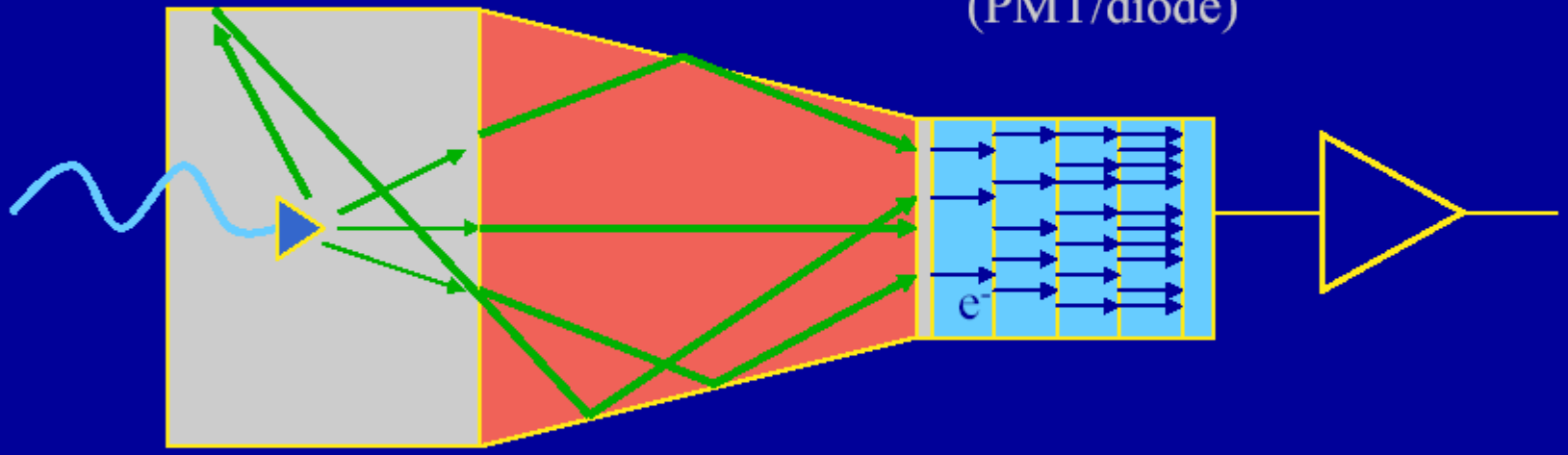

Scintillation crystal NaI (Tl)
0.5 MeV -> 3 eV γ's, ~12% efficiency

20,000 γ's

Light guide
80% efficient

16,000 γ's

Bialkali photocath.
20% efficient

3200 e^-

$\Delta E/E \sim 2.35*(1/\sqrt{3200}) = 4\%$ FHWM

The Energy Resolution of a SC is determined by the statistical fluctuations of the number of photoelectrons generated at the photocathode.

Advanced photocathodes like Bialkali (K-Cs) has maximum quantum efficiency of 25-30 % giving:

$$\frac{\Delta E}{E} = \frac{6\,keV}{60\,keV} = 0.1$$

only for small crystals, where nearly all photons are collected by the photocathode.

For large crystal area > 100 cm^2 even careful packing in Teflon foil will finally scatter half of the emitted photons:

$$\frac{\Delta E}{E} = 0.15 \qquad at \quad 60 \;\; keV$$

Reduction of internal background
mainly produced by charged particles:

1) well-type mounting of the detectors up to 100 cm^2
   - five sides anticoincidence material, for instance plastic foil,

Balloon missions,
SUZANKU

2) for large area detectors: several x 100 cm^2, since 1974 the so -called PHOSWICH, “phosphor sandwich” detectors are used (first on the orbit in 1975): detector crystal is optically coupled to a thick shielding crystal of different fluorescence decay time.

Both crystals are viewed by the same phototube.

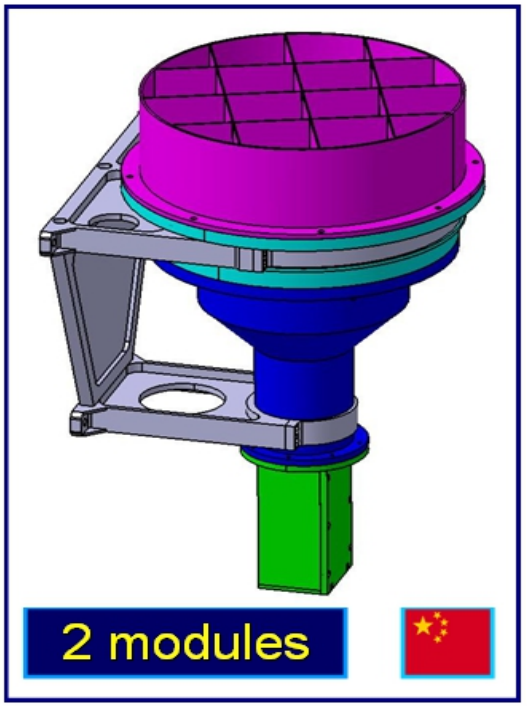

Collimateur (haut de 40 mm, épais de 1 mm)

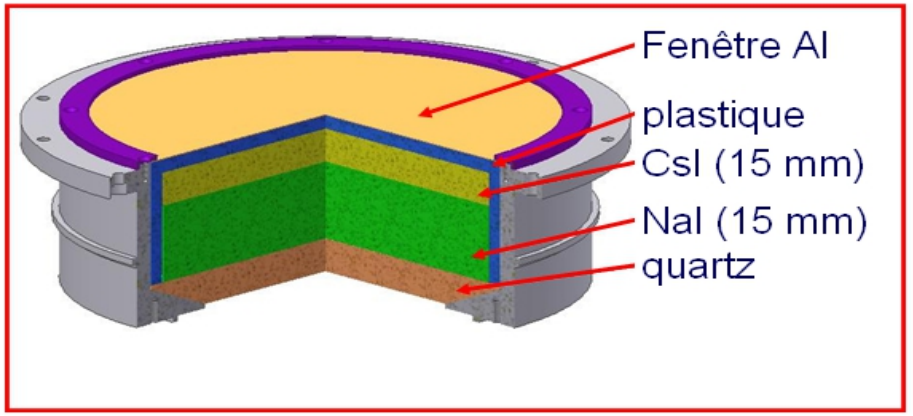

Surface utile : 280 cm^2 par module

Domaine spectral : 50 keV à 5 MeV

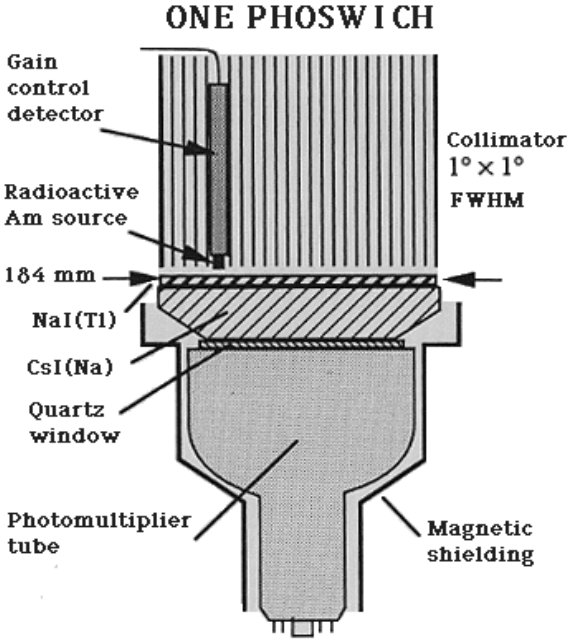

For large collecting area instruments:
SUZAKU – 16 main detectors,
40-600 keV, A_{coll}=404 cm^2

Commonly used in X-ray and Gamma - ray observatories, up to 100 GeVs.

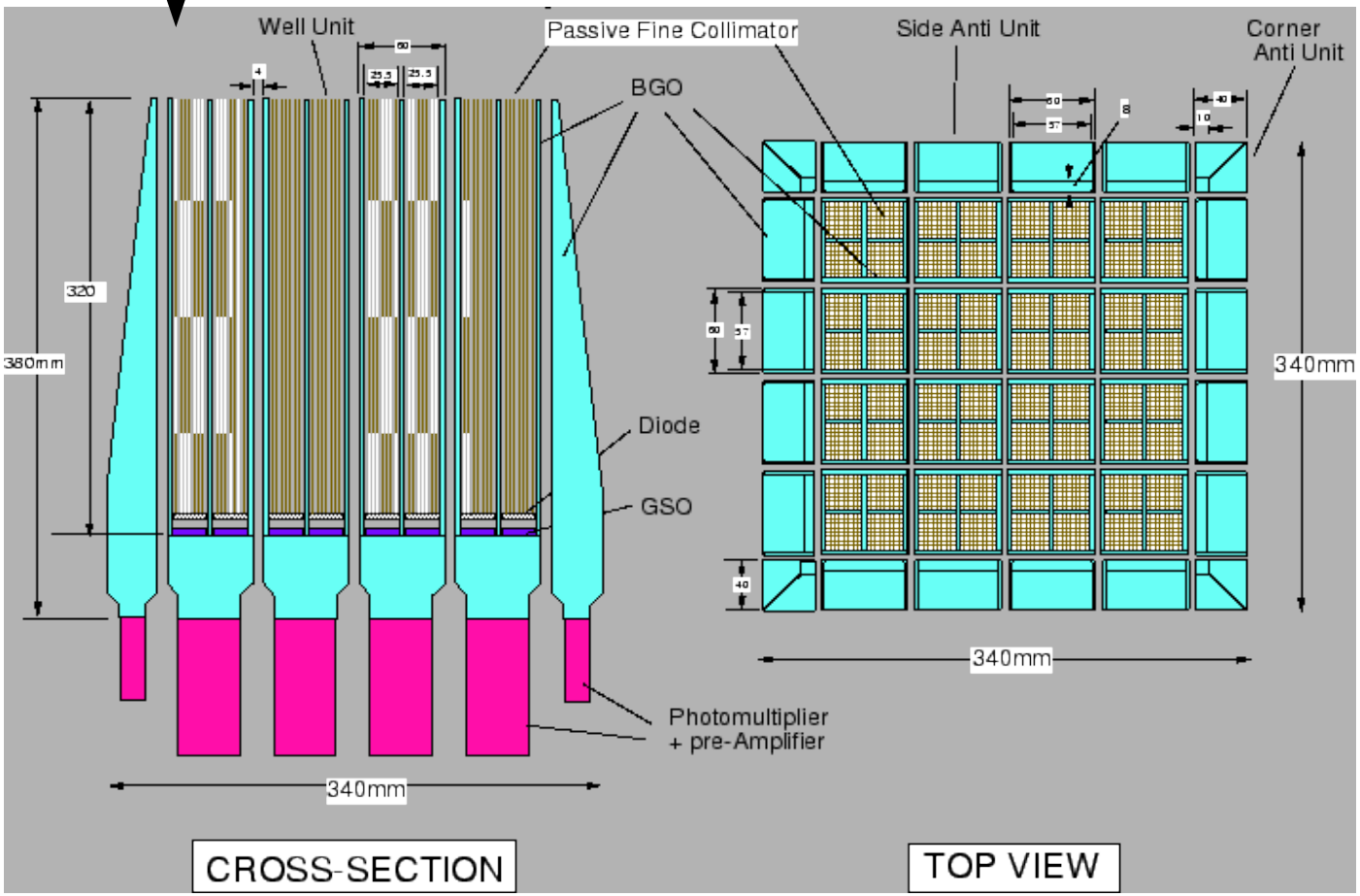

Imaging Proportional Counters: < 10 keV

Sensitivity increases by the use of
Imaging Optics and
Position Sensitive Focal Plane Detectors.

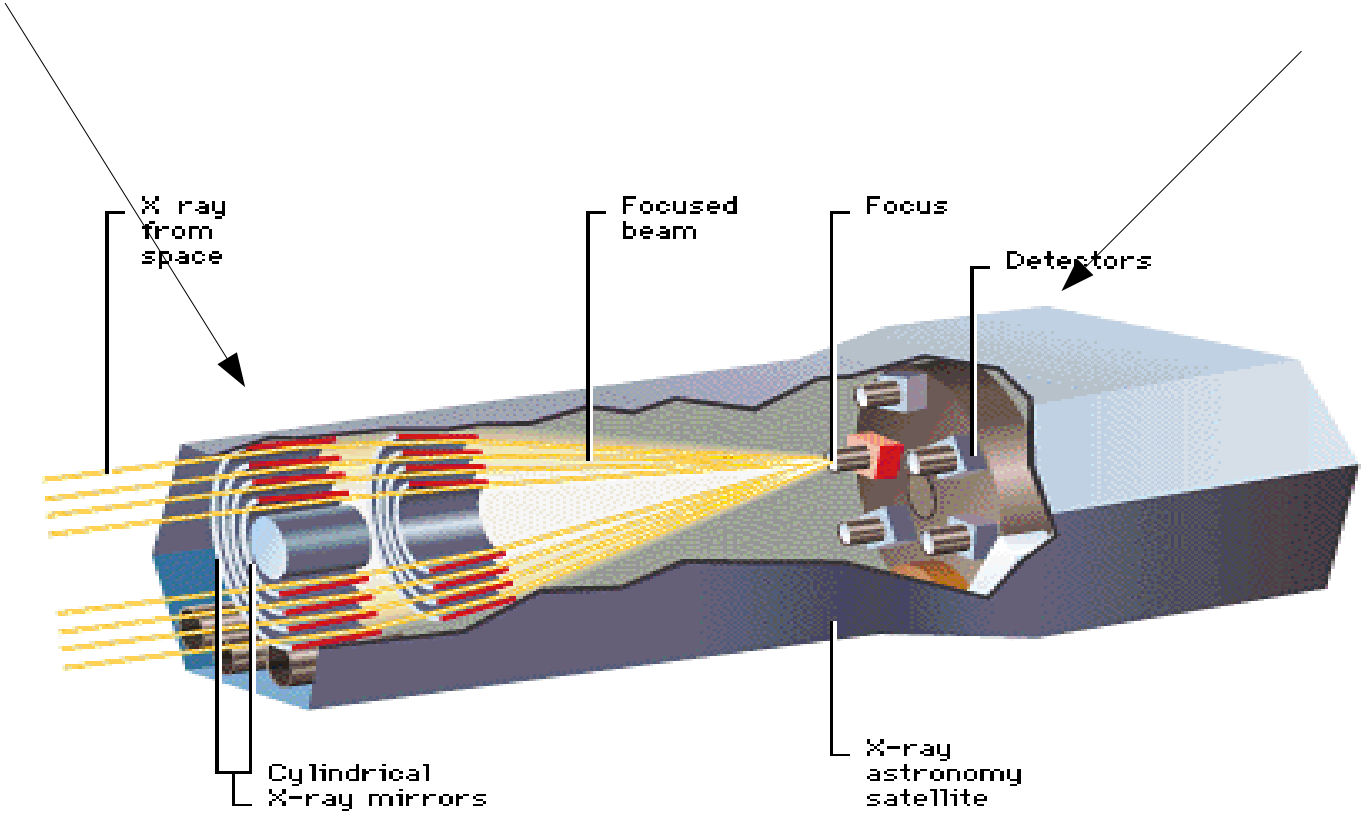

Mirror system gives 10 times higher effective collecting area than the large area PCs or SCs.

RXTE, INTEGRAL

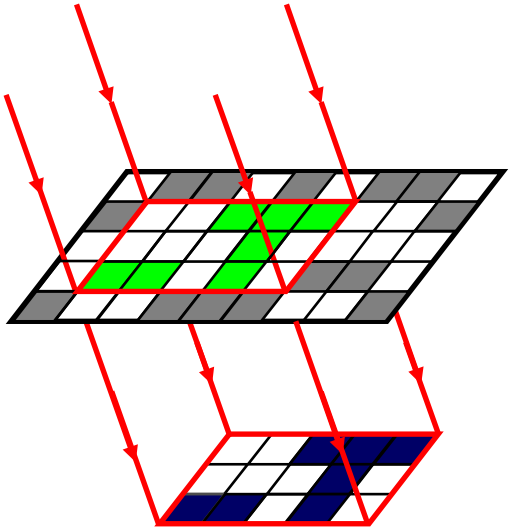

$$A_{eff} = A_{\det}$$

CHANDRA, XMM-Newton

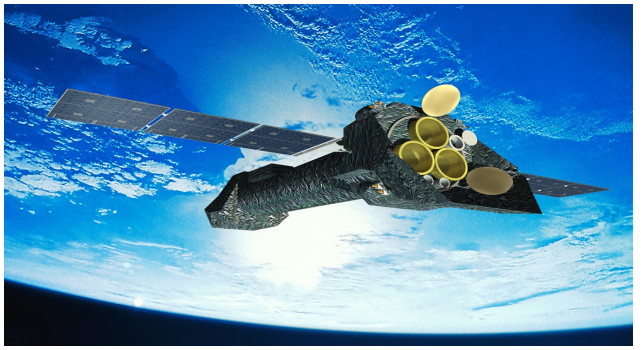

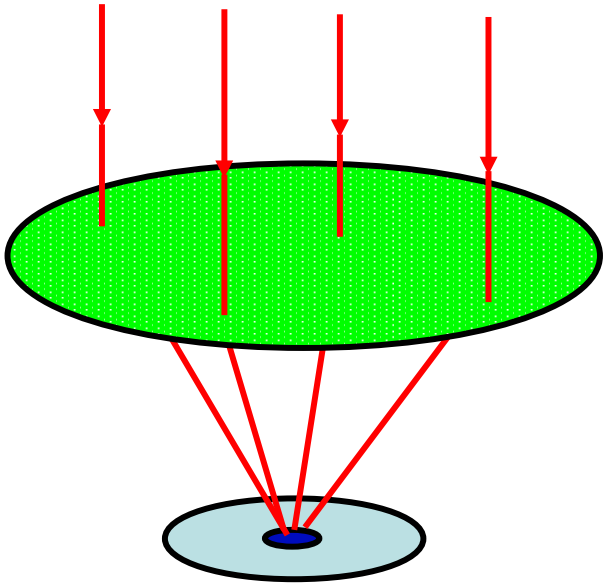

$$A_{eff} >> A_{\det}$$

Maximum energy of focused photons:

$$E_{max} \propto F,$$ where F is a focal length.

E_{max} = 10 keV for F = 2 m : CHANDRA, XMM-Newton

E_{max} = 70 keV for F = 10 m: NuSTAR

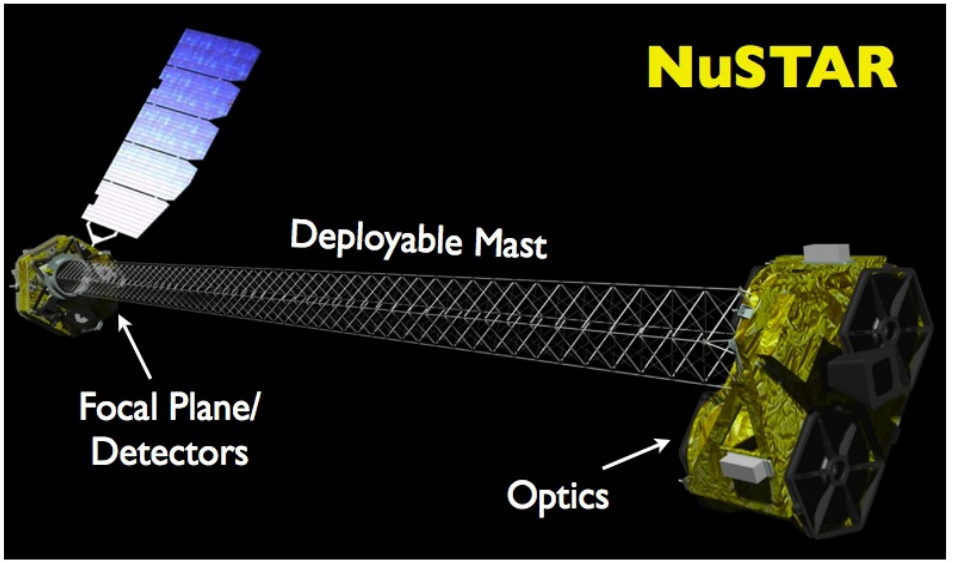

1) Imaging capability gives much better angular resolution.
2) Background detection is limited to an angular resolution element of the mirror-detector system.

ATHENA – Advenced Telescope for High ENergy Astrophysics, 2037???

The *Athena* X-ray observatory

Ariane 6
L1 orbit
4 years nominal mission
+ possible extensions
ToO response ≤ 4 hrs

X-ray Integral Field Unit:
ΔE: 2.5 eV
Field of view: 5 arcmin
Operating temperature: 50 mK

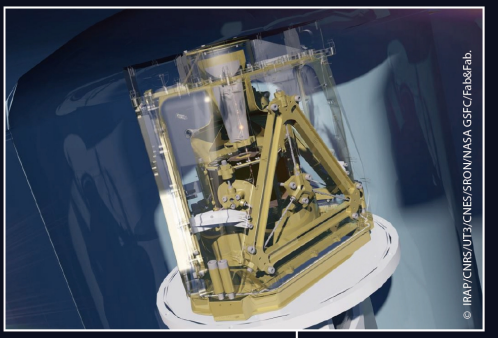

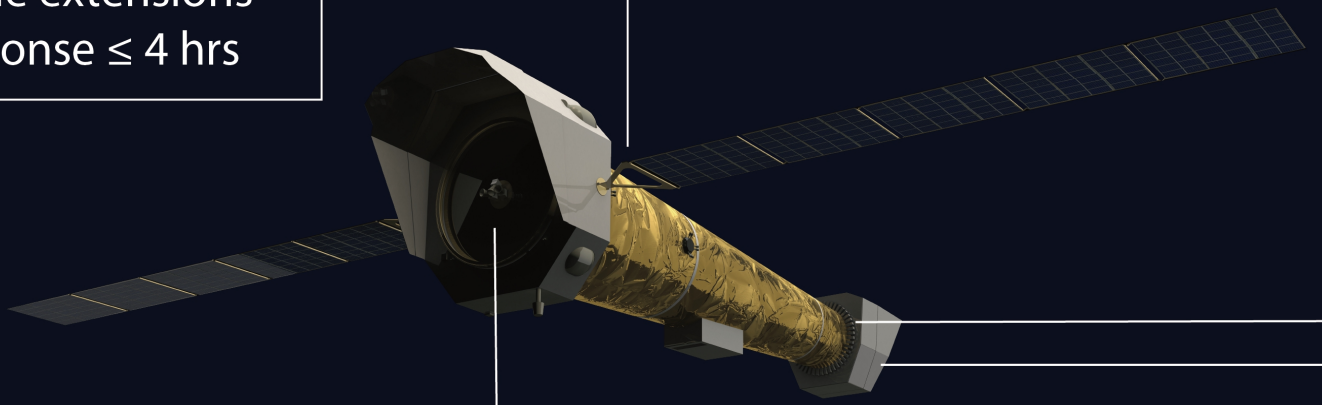

Silicon Pore Optics:
1.4 m^2 at 1 keV
5 arcsec HEW
Focal length: 12 m
Sensitivity: 3 10^{-17} erg cm^{-2} s^{-1}

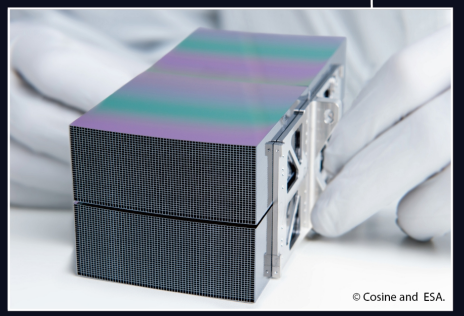

Wide Field Imager:
ΔE: < 80 eV at 1keV
Field of view: 40 arcmin
Small/Fast detector for bright sources

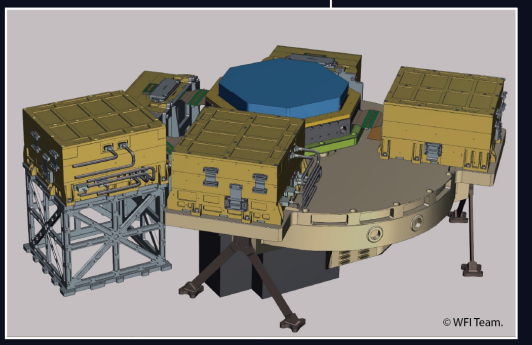

Fundamental questions - ATHENA mission

- How does the large scale structure in the Universe form and evolve?
- How do black hole grow and help shape the Universe?
- How and when are the chemical elements formed?

Athena is an observatory with ~500 projects/year:

- Stars, exoplanets, pulsars, neutron stars, gravitational wave events, galaxies
- Unprecedented discovery space

Principles of ranking the lecture:

- to be here

- to participate into discussions

- to make a homework

- hand – on sessions with the use of the computer.....

wi-fi password: a w sercu maj

HEASARC – High Energy Astrophysics Science Archive Research Center

http://heasarc.gsfc.nasa.gov/

HOMEWORK #1:

1-2 slides about the mission's detector in the nugget

Up to Nov. 8. 2022

send me by e-mail: agata@camk.edu.pl

NEXT LECTURE Nov. 3. 2022